STUDY OF SUBSTITUTED BENZENESULFONATE-CONTAINING LAYERED DOUBLE HYDROXIDES AND INVESTIGATION OF THE HEXAMETHYLENETETRAMINE ROUTE OF LDH SYNTHESIS

Sriram Ambadapadi, B. Pharm.

Thesis Prepared for the Degree of

MASTER OF SCIENCE

UNIVERSITY OF NORTH TEXAS

May 2007

APPROVED:

Paul S. Braterman, Major Professor
Mohammad A.Omary, Committee Member
Ruthanne Thomas, Chair of the Department of Chemistry
Sandra L. Terrell, Dean of the Robert B. Toulouse School of Graduate Studies

Ambadapadi, Sriram. Study of Substituted Benzenesulfonate-Containing Layered Double Hydroxides and Investigation of the Hexamethylenetetramine Route of LDH Synthesis. Master of Science (Analytical Chemistry), May 2007, 76 pp., 20 tables, 57 illustrations, chapter references, 104 titles.

Benzenesulfonates, para-substituted with amine, chloride and methyl groups were successfully incorporated into layered double hydroxides of two different compositions, 2:1 Mg-Al LDH and 2:1 Zn-Al LDH. These parent materials were also doped with small amounts of nickel and the differences in the two systems were studied.

The hexamethylenetetramine route of layered double hydroxide synthesis was investigated to verify if the mechanism is indeed homogeneous. This included attempting preparation of 2:1 Mg-Al LDH, 2:1 Zn-Al LDH and 2:1 Zn-Cr LDH with two different concentrations of hexamethylenetetramine. The analytical data of the products suggest that the homogeneous precipitation may not be the true mechanism of reaction involved in LDH synthesis by this method.

ACKNOWLEDGEMENTS

My first and profound thanks go to Prof. Paul S. Braterman for his advice and guidance during the period of my education in the Department of Chemistry at the University of North Texas. I will endeavor to sustain the knowledge I gained in his guidance and also to distribute it in my capacity.

Mickey C. Richardson, my colleague and friend has helped me learn the nuances of experimental methods in the chemistry lab. I thank him for his patience, attention and help.

My gratitude should also go Dr. Nandika D'Souza and her group members Laxmi kumari Sahu and Mithun Kamat for their collaboration in the benzenesufonates project.

I am also thankful to my thesis committee member and Dr. Mohammad Omary.

The agencies that have funded this work are NIST, Robert A. Welch foundation and UNT faculty research fund.

Thanks to my family for their love and support.

TABLE OF CONTENTS

Page

LIST OF TABLES

Page

LIST OF ILLUSTRATIONS

Page

CHAPTER 1

INTRODUCTION

The major part of this thesis is concerned with layered double hydroxides of various compositions and their properties. It is only apt, therefore, to include an introduction to layered double hydroxides along with a brief historical overview.

1.1. Structure and Composition

Layered double hydroxides (LDHs) as a class have been studied for over a century now, starting in the middle of the 19th century. By the year 1967 the structure of these materials was correctly identified and published [1-7]. They were found to contain both the divalent and trivalent metals in the sheets as shown in the schematic Figure 1.1. These materials have a general formula $[M^{II}_{1-x}M^{III}_{x}(OH)_{2x}]^{x+}(A^{n-})_{x/n}.mH_2O$ where M^{II} represents an divalent metal, M^{III} represents a trivalent metal and A^{n-} an anion. These materials are popularly known as hydrotalcite-like materials and anion exchanging clays. They are composed of brucite like layers in which a part of the magnesium ions is replaced by trivalent metal ions. These trivalent metal ions give the sheet a net positive charge, which the latter neutralize by housing anions in the interlayer space. Usually some amount of water is also found in the interlayer space along with the anions. The anions in the material are exchangeable with other anions and this property of anion exchange makes layered double hydroxides academically interesting and commercially valuable.

The charge density of the anion plays an important role in its capability to replace an anion in the interlayer space of the LDH. More the charge density more is the ion's exchanging capacity. The monovalent ions generally are easily replaceable with divalent ions and this is the

reason for making chloride or nitrate precursor for many LDHs with divalent anions. Many organic anions with comparatively large sizes are also intercalated into the LDH by making a chloride or nitrate precursor and exchanging it with these anions [8].

The metals in the layers are usually di and trivalent. There are exceptions to this and monovalent metals like lithium along with tetravalent metals like titanium were used to make some LDHs[8]. The divalent metal ions usually found in LDHs are Mg, Fe, Co, Ni, Cu, Zn, Ca etc and some usual trivalent metal ions are Al, Cr, Fe, Co, Ni, Ga, Ln etc[8].

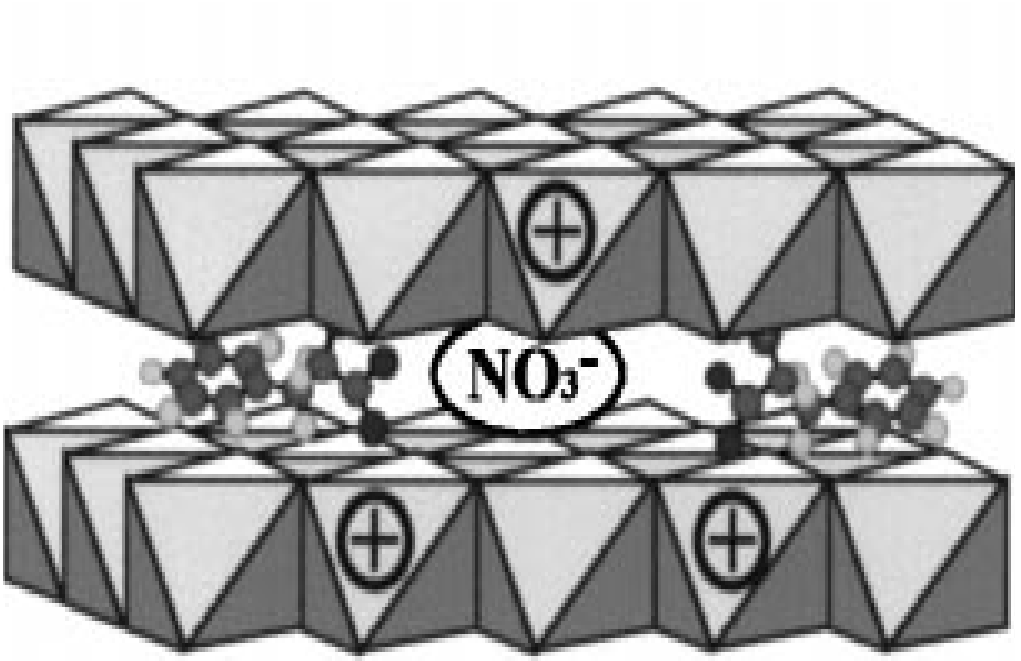

Figure 1.1: Schematic of typical layered double hydroxide. Two layers of the metal hydroxides can be seen in the figure. The interlayer space has nitrate and other anions in this figure. [Figure is taken from *Journal of Solid State Chemistry* 162, 52-62 (2001)].

1.2. Anions in the Gallery Space

The space between the two layers of metal sheets is called the interlayer space and the resultant distance when the thickness of the layers is subtracted from this is called gallery height. So, gallery height is the space the anions can occupy. The orientation of different anions in this space is different and is found to be dependent on their charge, structure and dimensions. LDHs

in nature usually contain carbonate and in some cases exist with chloride or sulfate as interlayer anions[9-15].

The anions present can be either monovalent like Cl^-, OH^-, NO_3^- or divalent like CO_3^{2-}, SO_4^{2-}, and some tetravalent groups like $[Fe(CN)_6]^{4-}$ [9,10, 16-23]

Small anions with greater symmetry like CO_3^{2-}, $NO3^-$ generally align themselves parallel to the brucite-like layers. The symmetry of the anions is found to be changing with the change in the trivalent metal concentration in the layers and this is to have maximum possible interaction between positive charges in the layers with negative charge of the anion. The Carbonate anion, existing in the D_{3h} symmetry changes to tilted C_{2V} in LDH with trivalent cation concentration reaching 0.44[24]. Nitrate on the other hand exists in tilted shape even in lower concentrations of trivalent cation due to its lower charge density compared to that of carbonate [25].

The tetrahedral anions like SO_4^{2-}, MoO_4^{2-}, CrO_4^{2-}, PO_4^{3-}, ClO_4^-, $CoCl_4^2$ and $NiCl_4^-$ can exist in either of the two possible ways of orientation, one of which is with the pyramidal portion lying perpendicular to the sheets in which three atoms face one sheet and one faces the other. ClO_4^- ions in LDH-ClO_4^- are in this orientation [26]. The other type is in which the C_2 axis of the tetrahedral structure is perpendicular to the sheets where two atoms face each sheet. SO_4^- ions in LDH- SO_4^- are in this orientation.

The octahedral $Fe(CN)_6^{3-}$, when present in the gallery distorts slightly and this is was explained to be because of the hydrogen bonds between cyanide nitrogen and the hydroxyl groups of the layers [27, 28].

When the intercalating anion is organic, which can be a carboxylate or a sulfonate the layers may contain between them a single layer or a double layer or even a partial overlap packing of the anion as the hydrophobic chains of the anions tend to attract each other in. The

nature of the packing depends both on the concentration of the anion and also the temperature of the reaction. Single layer is favored when the ratio of the anion to the trivalent metal is close to 1. A bilayer results when this ratio of the organic compound and the trivalent metal is more than one i.e., in the presence of excess interlayer species. [29-32] (This condition can arise when neutral molecules such as carboxylic acids are incorporated even at high pH conditions [31].)

The substituted benzene sulfonates, the anions for the LDH for the major part of this thesis, when in the interlayer are believed to be standing erect with the negative charge towards the layers of the LDH, and the sulfate group hydrogen bonded to the layer hydroxides.

1.3. Synthesis

There are many procedures by which LDHs can be obtained, among which the direct precipitation method is the most commonly employed one, for, it is simple and reliable. In this method the common solution of metal salts is added with the required alkali. 50%w/w sodium hydroxide is very useful for this, in that it avoids the transfer of carbonate formed in it into the LDH as it is precipitated out of the solution because of common-ion effect.

When aluminum is the trivalent metal in this method, aluminum hydroxide forms as an intermediate which is then acted upon by more alkali to produce LDH. This is reflected in the titration plot as an additional plateau.

LDHs with Cr (III) as the trivalent cation show a different path in their formation. They show a single plateau which corresponds to the pH of formation of the LDH.

There are numerous modifications of direct method of LDH synthesis which include coprecipitation, a technique in which all the cations and anion precipitate in the solution simultaneously at a constant pH [33-35].

The material obtained from the above mentioned methods is poorly crystalline in nature and can be improved by certain techniques which involve employing increased temperatures. This process is called 'aging' and is usually done by gentle reflux at a temperature of 90-100^{0}C for 24hrs. This improves the crystallinity through Ostwald ripening [36-38] in which large crystallites form by dissolution of small particles and their reformation.

Hydrothermal treatment [39-42] also yields materials of improved crystallinity. This method is employed in the preparation of materials discussed in Chapter 4. In this method the common solution of salts along with the alkali is heated above 120^{0}C in a sealed vessel. This helps in dissolution and recrystallization of LDH during its formation.

1.4. Anion Exchange

One of the most common names of LDH is 'anionic clays' and this is so because they are excellent exchangers of anions. This exchange of the interlayer anion for another anion of choice in solution is undoubtedly the single most important feature of LDH research around the world. The only condition an anion has to satisfy to be able to be incorporated into LDH is that its area per unit charge should not be greater than the area per unit charge of the LDH sheet [43-45].

Different kinds of anions are incorporated into the LDH by anion exchange method. For this, an LDH precursor with nitrate or chloride ion is prepared which is then made to exchange its anion with the anion of choice. This exchange is a simple process in which the LDH precursor is dispersed in water and stirred with a solution containing excess of the required anion. The order of preference of exchangeable anions can be given as [40, 46, 47]:

$$NO_3^- < Br^- < Cl^- < F^- < OH^- < MoO_4^{2-} < SO_4^{2-} < CrO_4^{2-} < HAsO_4^{2-} < HPO_4^{2-} < \text{Napthol Yellow}^{2-} < CO_3^{2-}$$

1.5. Thermal Properties

Layered double hydroxides are unstable at moderately high temperatures and their structure was found to collapse upon heating. Thermogravimertric analysis (TGA) of LDH samples shows that they lose about 30-40% weight upon heating to 500^0C. This weight loss is due to the fact that they lose physically adsorbed water, water in the interlayer space, hydroxides of the sheets and the interlayer anions in gradual and individual steps. These calcined products recover to some extent upon exposure to moist air or when immersed in aqueous solutions containing anions [48-51].

The surface water starts to come out of the material at about 100^0C and this step is complete when the temperature reaches 105^0C. Miyata [52, 53] proposed that the loss of interlayer water is responsible for the weight reduction step around temperature 280^0C which can be observed on a differential thermal analysis (DTA) plot. This and other observations about the thermal properties of the LDHs are for the Mg Al LDH with carbonate as interlayer anion. LDHs with different anions show different thermal behaviors as these patterns depend on their anions and the atmospheric conditions under which the study is conducted.

The other distinct features in the DTA of carbonate LDH occur at 400^0C and 450^0C. They can be attributed to loss of structural hydroxide groups and the interlayer carbonate respectively[54]. Increasing the calcination temperature to about 500^0C highly disordered MgO is obtained. This disorder may be because it has some amount of Al^{3+} in it. Upon increasing the temperature to about 1000^0C well crystallized MgO along with $MgAl_2O_4$ spinel is formed [55-57].

1.6 References

1. Mortland,M.M.; Gastuche, M.C. *Compt Rend.* **1962**, *225*, 2131-2133.
2. Ross, G.S.; Kodama, H. *Am. Mineral.* **1967**, *52*, 1036-1047.

3. Ingram, L.; Taylor, H.F.W. *Mineral Mag.* **1967,** *36*, 465-479.

4. Allmann, R. *Am. Mineral.* **1968,** *53,* 1057-1058.

5. Van Oosterwyck-Gastuche, M.C.; Brown, G.;Mortland, M.M. *Clay. Miner.* **1967**, *7*, 177-192.

6. Brown, G.; Van Oosterwyck-Gastuche, M.C. *Clay. Miner.* **1967**, *7*, 193-201.

7. Allmann, R. *Chimia*. **1970**, *24*, 99-108.

8. Rives, V.; Layered double hydroxides, Huntington, Newyork; Nova science publishers, Inc, 2001.

9. Brindley, G.W.; Kikkawa, S. *Amer.Mineral.* **1979**, *64*, 836.

10. Drits, V.A.; Sokolova, T.N.; Sokolova, G.V.; and VI.; and Cherkashin, *Clays. Clay Miner.* **1987**, *35*, 401.

11. Kashaev, A.A.; Feoktistov, G.D.; Petrova, S.V. *Zapisky Vsesouzngo Mineralogitcheskogo Obchestva*, **1982**, *11*, 121.

12. Bish, D.L.; Lvingstone, A. *Miner. Mag.* **1981**, *44*, 339.

13. Nickel, E.H.; Wildman, J.E. *Miner. Mag.* **1981**, *44*, 333.

14. Cooper, M.A.; Hawthorne, F.C.; *Canadian Mineralogist* **1996**, *34*, 91.

15. Nickel, E.H. *Miner. Mag.* **1976**, *40*, 644.

16. Allmann, R.; *Neues Jahrb. Miner Monatsh.* **1969**, 552.

17. Allmann, R.; *Neues Jahrb. Miner Monatsh.* **1977**, 136.

18. Bish, D.L.; *Bull. Minera.l* **1980**, *103*, 170.

19. Korting, S.; *Z. Freunde Miner.* **1976**, *27*, 53.

20. Miyata, S.; *Clays Clay Miner.* **1983**, *31*, 305.

21. Miyata, S.; Okada, A.; *Clays Clay Miner.* **1977**, *25*, 14.

22. Schutz, A.; Biloen, P. *J.Solid State Chem.* **1987**, *68*, 360.

23. Miyata, S.; *Clays Clay Miner.* **1975**, *23*, 369.

24. Labajos, F.M.; Rives, V.; Ulibarri, M.A. *Spectrosc. Lett.* **1991**, *24*, 499-508.

25. Xu, Z.P.; Zeng, H.C.; *J.Phys Chem.* **2001**, *105*, 1743-1749.

26. Brindley, G.W.; Kikkawa., S.; *Clays Clay Miner.* **1980**, *28*, 87-91.

27. Braterman, S.; Tan, C.Q.; Zhao, J.X.; *Mater. Res.Bull.* **1994**, *29*, 1217-1221.

28. Kikkawa, S.; Koizumi, M.; *Mater. Res.Bull.* **1982**, *17*, 191-198.

29. Carlino, S.; *Solid State Ionics.* **1997**, *98*, 73-84.

30. Kanoh, T.; Shichi, T.; Tagaki, K; *Chem. Latt.* **1999**, 117-118.

31. Xu, Z.P.; Braterman, P.S.; Seifollah, N.; Self Assembly and Multiple Phases in ZnAl-Stearate-Layered Double Hydroxides. 224th ACS National Meeting, Boston, MA, **2002.**

32. Clearfield, A.; Kieke, M.; Kwan, J.; Colon, J.L.; Wang, J.; *J. Inclusion Phenom. Mol. Recognit. Chem.* **1991**, *11*, 361-378.

33. Brocker, F.J.; Dethlefsen, W.; Kaempfer, K.; Marosi, L.; Schwarzmann, M.; Tribskorn, B.; Zirker.; German Patent 2,255,909,1972.

34. Miyata, S.; Kumura, T.; Shimada, M.; German Patent 2,061,156, 1970.

35. Woltermann, G.M. US Patent 4,454,244, 1984.

36. Ostwald, W. *Z. Phys.Chem.* **1897**, *22*, 289.

37. Boistelle, R.; Astier, J.P.; *J. Cryst. Growth.* **1988**, *90*, 14-30.

38. Henisch, H.K.; Crystals in Gels and Liesegang Rings : in vitro veritas. New York: Cambridge University Press, 1988.

39. Cavani, F.; Trifiro, F.; Vaccari, A.; *Cat. Today.* **1919**, *11*, 173-301.

40. Trifiro, F.; Vaccari, A. *In.Comprehensive Supramolecular Chemistry.* New York: Pergamon, **1996**, 251-291.

41. Hickey, L.; Kloprogge, J.T.; Frost, R.L.; *J. Mater. Sci.* **2000**, *35*, 4347-4355.

42. Newman, S.P.; Jones, W. *New J.Chem.* **1998**, *22*, 105-115.

43. Boclair, J.;Themodynamic and structural studies of layered double hydroxides. PhD Dissertation, University of North Texas, Denton, Tx, **1998**.

44. Richardson, M.; Braterman, P.S.; Yarberry, F.; Xu, Z.P. Metallocyanide / Carbonate Layered Double Hydroxide Competition. Unpublished work. University of North Texas, Tx, **2002**.

45. Carrado, K.A.; Forman, J.E.; Botto, R.E.; Winans, R.E. *Chem. Mater.* **1993**, *4*, 472-478.

46. Yamaoka, T.; Abe, M.; Tsuji, M. *Mater. Res. Bull.* **1989**, *24*, 1183.

47. Miyata, S.; *Clays Clay Miner.* **1983**, *31*, 305-311.

48. Sato, T.; Kato, K.; Endo, T.; Shimada, M. *Reactivity Solids* **1986**, *2*, 253

49. Chibwe, K.; Jones, W. *J.Chem. Soc., Chem. Comm.* **1989**, 926.

50. Kwon, T.; Pinnavaia, T.J. *Chem. Mater.* **1989**, *1*, 381.

51. Rocha, J.; del Arco, M.; Rives, V.; Ulibarri, M.A. *J. Mater. Chem.*. **1999**, *9*, 2499.

52. Miyata, S. *Clays Clay Miner.* **1980**, *28*, 50.

53. Miyata, S.; Okada, A.; *Clays Clay Miner.* **1977**, *25*, 14.

54. Yun, S.K.; Pinnavaia, T.J. *Chem. Mater.* **1995**, *7*, 348.

55. Pesic, L.; Salipurovic, S.;Markovic, V.; Vucelic, D.; Kagunya, W.; Jones, W. *J.Mater. Chem.* **1992**, *2*, 1069.

56. Rey, F.; Fornes, V.; Rojo, J.M. *J. Chem. Soc., Faraday Trans.* **1992**, *88*, 2233.

57. Labajas, F.M.; Rives, V.; Ulibarri, M.A. *J. Mater.Sci.* **1992**, *27*, 1546.

CHAPTER 2

TECHNIQUES EMPLOYED

This chapter is dedicated to introducing the techniques employed for the characterization of the materials synthesized for the research.

2.1 X-ray Diffraction (XRD)

Powder X-ray diffraction is the main identification tool for the layered double hydroxides (LDHs) as it gives the information about the crystal structure of the material, which can be compared to the known patterns to identify the material. The typical XRD patterns of LDHs with common anions show the diffraction planes indexed in $3R_1$[1-3]. Based on crystallographic evidence we assume rhombohedral structure for the LDHs and the usual basal spacings as d_{003}, d_{006}, d_{009} etc which correspond to the interlayer spacing are obtained from the XRD pattern of a material and each of them can give us the exact interlayer spacing upon multiplication with an appropriate integer. The non-basal spacings like d_{110} give the measure of the parameter 'a'.

The X-ray diffraction pattern of a substance is unique for it and thus finding exact match of pattern often means establishing the identity of the substance. The XRD is based on Bragg's law[4]:

$$n\lambda = 2d * \sin\theta$$

where λ is the wave length of the x-ray beam, d is the interplanar distance, θ is the angle between the incident x-ray and the reflecting crystal plane, and n is an integer representing the order of reflection (in crystallography, by convention n=1). The condition for a crystal to reflect x-rays, according to Bragg's law is that the sine of angle of incidence, $\sin\theta = n\lambda/2d$.

2.2 Infrared Spectroscopy

Infrared spectroscopy is another important tool for the characterization of layered double hydroxides [5-9]. Although it is not sufficient to fully characterize the materials, it is very useful, for some peaks give valuable information. LDH materials with different divalent and trivalent metals in their sheets show some specific peaks in their infrared spectrum. For example the aged 2:1 Mg-Al LDH has a distinct and characteristic peak around 444 cm-1, aged 2:1 Zn-Al LDH has one around 425 cm^{-1}. These peaks are absent or very weak in fresh spectra and thus can help us in distinguishing between fresh and aged materials [10-12].

The typical peaks observed for common inorganic anions are well reported and help us identify the compound unequivocally. The peaks at 1350-1380 cm^{-1} and 670-690 cm^{-1} for example are proofs for the presence of carbonate in the LDH. Similarly peaks around 1384 cm^{-1}, 830 and 750 cm^{-1} are indicative of nitrate. Other inorganic anions like sulfate, ferrocyanide, silicate, ferricyanide, show their characteristic vibration bands in the mid-infrared region.

Infrared spectroscopy is especially useful for the organic interlayer ions as it is well established that it is a standard technique for identification of organic functional groups like CH, CN, COO, CC, SO_3, OSO_3, and NO_2. Cations present in the layers and the hydrogen bonding exhibited of some of these ions tend to cause these peaks to shift a bit, however.

2.3 Atomic Absorption Spectroscopy (AAS)

Atomic absorption spectroscopy is a common technique for the identification of metal concentration in the material under analysis. It is based on the fact that ground state metals absorb light at specific wavelengths. So, the metals in the solution state are converted to their ground state selves by passing them through the flame. Light of appropriate wavelength is then

supplied and the amount of this light absorbed by the metal is measured. It is a simple and efficient technique for an LDH chemist as it gives the concentrations of divalent and trivalent metals present in its layers. It also gives information about the metallic anion groups that can be present in the interlayer.

The metals ratio in the layer is very important for the LDH chemistry and this when combined with the CHN analysis gives a nominal chemical formula for the material being analyzed.

2.4 Thermogravimetric Analysis (TGA)

Thermogravimetirc analysis is the technique in which the change in weight of the material under analysis is measured under conditions of changing temperature. It gives the behavior of the material under elevated temperatures. Usually the weight loss percentage is plotted against temperature in TGA. The differential of this weight loss called DTA gives us the temperatures of peak weight losses which can then be interpreted depending upon the material under study.

Layered double hydroxides are often tested for their behavior under different temperature conditions to understand their stability and effectiveness as catalysts or additives. The common weight reduction points we see in the DTA of a layered double hydroxide correspond to loss of adsorbed water, dehydroxylation which is the loss of hydroxyl groups in the layers causing the structure to collapse and the one corresponding to the loss of interlayer anion.

A carefully weighted amount of the material is analyzed by TGA under atmospheres of inert gases like N_2 or under air to observe the behavior of the material in those atmospheres respectively. Layered double hydroxides usually yield the oxides of the metals present in the

layers upon heating up to 500^0C (MgO for example) and up on heating further to 1000^0C give spinels (such as $MgAl_2O_4$).

2.5. References

1. Trifiro, F.; Vaccari, A. *In.Comprehensive Supramolecular Chemistry.* New York: Pergamon, **1996**, 251-291.
2. Bookin, A.S.; Drits, V.A. *Clays Clay Miner.* **1993**, *41*, 551-557.
3. Bookin, A.S.; Cherkashin, V.I.; Drits, V.A. *Clays Clay Miner.* **1993**, *41*, 558-564.
4. Lipson, H.; Steeple, H. *Interpretation of X-ray Powder diffraction Patterns.* St.Martin's Press, New York, **1970**, pp 32.
5. Clark, R.J.H.; Huster, R.E. in *Spectroscopy of Inorganic-based Materials; Vol.14,* John Wiley & Sons, New York, **1987**.
6. Henning, O. in *The Infrared spectrum of Materials*; Farmer, V.C Ed.; Mineralogical Society: London, **1974**, Chapter 19.
7. Sakuri, T.; Sato, T.; Yoshinaga, A. *Proc. 5th Int. Symp. Chem. Cem., Tokyo*, **1968**, Vol.1, pp 300-321.
8. Ortego, J.D.; Jackson, S.; Yu, G.; McWhinney, H.; Cocke, D.L. I. *J.Environ. Sci. Health,* **1989**, A24(6).
9. Mollah, M.Y.A.; Tsai. Y.N.; Hess, T.R.; Cocke, D.L. *J. Hazardous Materials*, **1992**, 30(3), 273-283.
10. Xu, Z.P.; Zeng, H.C.; *J.Phys Chem.* **2001**, *105*, 1743-1749.
11. Bookin, A.S.; Cherkashin, V.I.; Drits, V.A. *Clays Clay Miner.* **1993**, *41*, 558-564.
12. Bookin, A.S.; Drits, V.A. *Clays Clay Miner.* **1993**, *41*, 551-557.
13. Kandall, D.N. *Applied Infrared Spectroscopy;* Chapman & Hall Ltd. London, **1966.**
14. Durig, J.R. in *Chemical, Biological and industrial Application of Infrared Spectroscopy;* John Wiley & Sons, New York, **1985**.

CHAPTER 3

INTERCALATION OF SULFONATES INTO THE Mg-Al AND Zn-Al LDH NITRATE PRECURSORS AND ANALYSIS OF THE PRODUCTS

3.1 Introduction and Motivation for the Work

Intercalation of sulfonates into layered double hydroxides (LDHs) and their characterization is well documented [1-4]. The anions *p*-toluene sulfonate and 4-chlorobenzenesulfonate which are discussed in this chapter were intercalated into LDHs prior to this work also [6-10]. The motivation for the use of these specific anions for the research is the idea of synthesizing a set of compounds which when blended with some polymers like PET act as flame retardants [11].

This part of the thesis deals with the synthesis and analysis of 2:1 Zn-Al and 2:1 Mg-Al LDHs with three different anions. The anions used for this purpose are benzene sulfonic acids [1-4] para substituted with amine (in the case of sulfanilic acid), with methyl group (in the case of *p* -toluenesulfonic acid) and with chloride (in the case of 4-chlorobenzenesulfonic acid). These LDHs were also altered from the parent by doping them with nickel to replace a fraction of the divalent metal present, which is either magnesium or zinc and their properties were also studied. Data for the doped materials are presented in tandem with that of the parent for the purpose of comparison and for evaluating the merits of nickel doping in flame retardation.

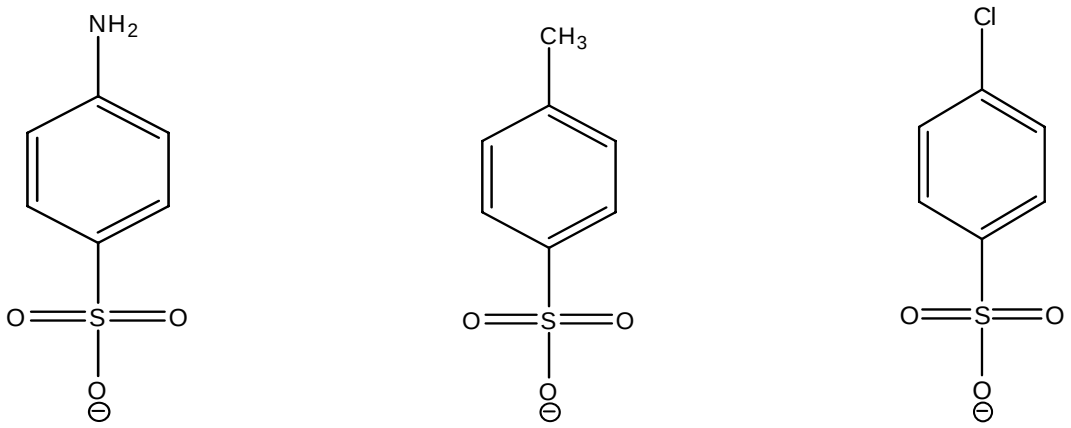

Figure 3.1: (a) Sulfanilate anion (b) *p* -toluenesulfonate anion (c) 4-chlorobenzenesulfonate anion.

3.2 Starting Materials

All the materials used in the synthesis of the LDHs that will be discussed here are obtained from the manufacturers and listed in Table 3.1 along with their grades. The materials were used as they were bought i.e. without further purification. The sulfonic acids were neutralized with sodium hydroxide to get their sodium salts and were isolated in the way described later in the chapter, before they were used for exchange. The water used was freshly purified by 'Milli-Q academic' (18MΩ cm^{-1}).

3.3 Synthesis

Preparation of LDHs was done in a two step procedure where the first step was to make the LDH with nitrate as the anion and the second to exchange this nitrate with the desired sulfonate anion.

Table 3.1 Chemicals used for the synthesis of compounds studied and their sources.

Name	Grade	Supplier
$Al(NO_3)_3.9H_2O$	98.-102%	Alfa Aesar
$Mg(NO_3)_2.6H_2O$	98%	Alfa Aesar
$Zn(NO_3)_2.6H_2O$	98%	Sigma-Aldrich
$NiCl_2.6H_2O$	ReagentPlus	Sigma-Aldrich
NaOH	50%w/w aq. Soln.	Alfa Aesar
Sulfanilic acid	99%, A.C.S. reagent	Sigma-Aldrich
p-toluenesulfonic acid	99%	Acros Organics
4-chlorobenzenesulfonic acid	Tech, 90%	Aldrich

In the preparation of LDH nitrate the trivalent and divalent metals salts of nitrate calculated to give 25gm of LDH were dissolved together in water to get 0.1M and 0.3M concentrations respectively. This solution of metal salts was heated to 40^0C and then 50%w/w sodium hydroxide was added to the solution for neutralization. The ratio of hydroxide added to the Al in the LDH is 6:1 as there are six moles of hydroxide per each 2:1 LDH. This mixture was refluxed at a temperature of 90-100^0C for 24hr under a nitrogen gas blanket with continuous stirring. After 24hr the LDH slurry is allowed to cool for a while and then it is centrifuged to separate LDH from the mother liquor. LDH thus obtained is not entirely free from the ions in the mother liquor and so it was washed twice with water, again by centrifugation. Initially a 3:1 ratio of divalent metal to trivalent metal was taken for the preparation of 2:1 LDH because the excess divalent metal acts a buffer for the changes in pH occurring during the titration.

In the second step, the LDH nitrate was dispersed in water and a solution of the sulfonic acid salt (anion of choice for the exchange), which has same number of moles of salt (twice the

number in case of sulfanilate) as there are of nitrate in the LDH, was added to it while stirring the slurry thoroughly. The stirring of the slurry was continued under continuous nitrogen flow for about an hour before it was centrifuged and washed twice. The obtained LDH with the desired anion was then dried in a large watch glass in the hot air oven at a temperature of 70^0C, ground and stored for analysis.

The salts of sulfonic acids were made in the laboratory by neutralizing the acids with required amount of 50%w/w Sodium hydroxide. For this the solution of sulfonic acid in water containing as many moles of acid as there are those of aluminum in the LDH was titrated with equal number of moles of sodium hydroxide. The salt was then isolated using a Rotovap and then its solution in water was made and used for the exchange.

A third step was also carried out in the preparation of nickel doped samples, which was incorporation of a small amount of nickel into the LDH. For this purpose, a solution of nickel chloride which was equimolar to the Al in LDH was added to the LDH of the required anion dispersed in water. This mixture was also stirred for an hour and then centrifuged and washed twice before it was dried and stored.

3.4 Results

3.4.1 Sulfanilate

The sulfanilate for the exchange was obtained by neutralizing the sulfanilic acid from the manufacturer with required amount of 50%w/w sodium hydroxide.

a. 2:1 Mg-Al LDH Sulfanilate

The exchange of the nitrate in the LDH was not complete with 1:1 ratio of sulfanilate to

nitrate. The ratio had to be increased to 2:1 to get reasonably complete exchange. The reason for this can be that sulfanilate is much less soluble in water and hence the amount of anion available in the solution is always limited. Intercalation of sulfanilate into LDH was not done prior to this work. The infrared spectrum sodium sulfanilate[5] given in Figure 3.2 shows sharp peaks at 1033, 1174 and 1224 cm^{-1}, for the symmetric and asymmetric S=O; sharp peaks at 1008, 1123 and 1502 cm^{-1} for the aromatic CH groups and the aromatic C=C. The assymetrical and symmetrical stretching modes of NH^{3+}occurring at 1572 and 1541 cm^{-1} in the sulfanilic acid are not expected to be present in its sodium salt [5]. The presence of sulfanilate in the LDH is confirmed by matching the infrared spectral peaks of sodium sulfanilate in Figure 3.2 to those in the LDH infrared spectra in Figure 3.3. The presence of 2:1 Mg-Al LDH is confirmed by the peak around 444 cm^{-1}. The peak around 1384cm^{-1} in Figure 3.3, though less prominent than in the infrared spectrum of the nitrate precursor, given in Figure 3.4 is evidence that some amount of nitrate remains in the product even after exchange. This is a common occurrence in LDH exchange reactions because some of the nitrates are caught between neighboring anions or water molecules and are not available for exchange. This peak can be seen in all of the LDH spectra that will be presented in this chapter. The peak at 1384cm^{-1} is indicated by asterisk mark in all the infrared spectra provided in the chapter to act as reference with the parent LDH and give an estimation of extent of exchange that took place.

The 2:1 Mg-Al LDH sulfanilate was further altered by incorporating some nickel in it. The infrared spectrum of this material is shown in the Figure 3.7. The infrared spectra of the Mg Al LDH sulfanilate with and without nickel doping look almost the same and both of them have the peaks around 444 cm^{-1}, indicating that the $Mg_2Al(OH)_6$ framework is intact [10]. This can be due to the fact that the amount of nickel getting into the LDH was small and the ratio of Mg to

Ni was nowhere near 1:1. Atomic absorption data given in the Table 3.2 of these materials also confirm this idea. The measured ratios of metals are seldom round figures and in the case of Mg Al LDH they are closer to 2, but the materials will be referred to as 2:1 materials throughout the chapter for the sake of convenience and to avoid confusion.

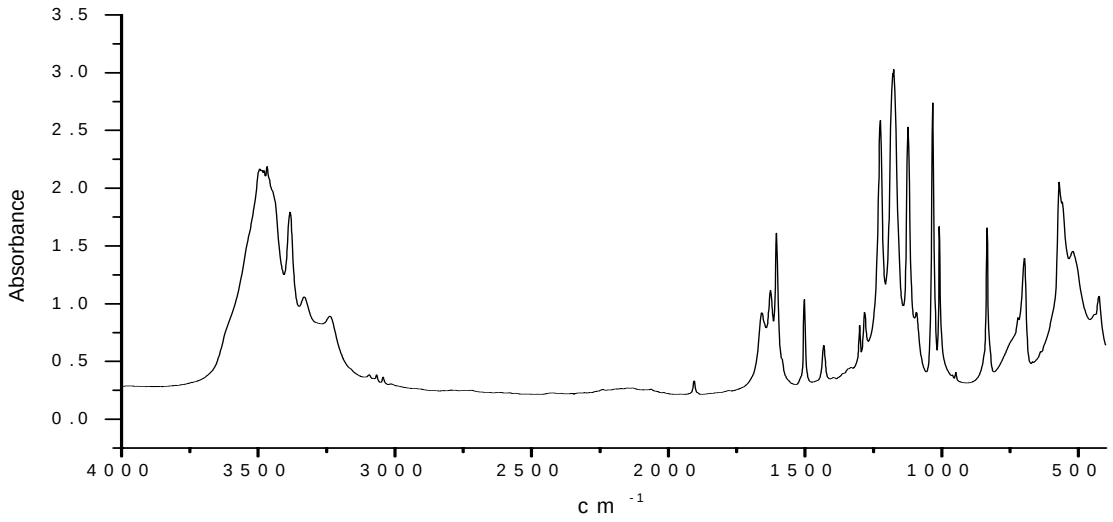

Figure 3.2: FTIR spectrum of sodium sulfanilate.

Table 3.2: Atomic absorption spectroscopy data and elemental analysis data for 2:1 Mg-Al LDH sulfanilate with and without nickel (for the elemental analysis, T stands for theoretical and E stands for experimental).

LDH Sample	**%Mg**	**%Al**	**%Ni**	**Mg : Al**	**Mg : Ni**	**(Mg+Ni:Al)**
Mg-Al Sulf	11.4	7.0	-	1.8:1	-	1.8:1
Mg-Al Sulf-Ni	13.2	7.0	3.3	2.1:1	9.7:1	2.2:1

LDH Sample	**%N_T**	**%N_E**	**%C_T**	**%C_E**	**%H_T**	**%H_E**	**%S_T**	**%S_E**
Mg-Al Sulf	3.62	3.96	18.67	13.12	4.17	3.62	8.31	4.40
Mg-Al Sulf-Ni	3.66	2.05	18.80	11.55	4.21	3.75	8.37	4.27

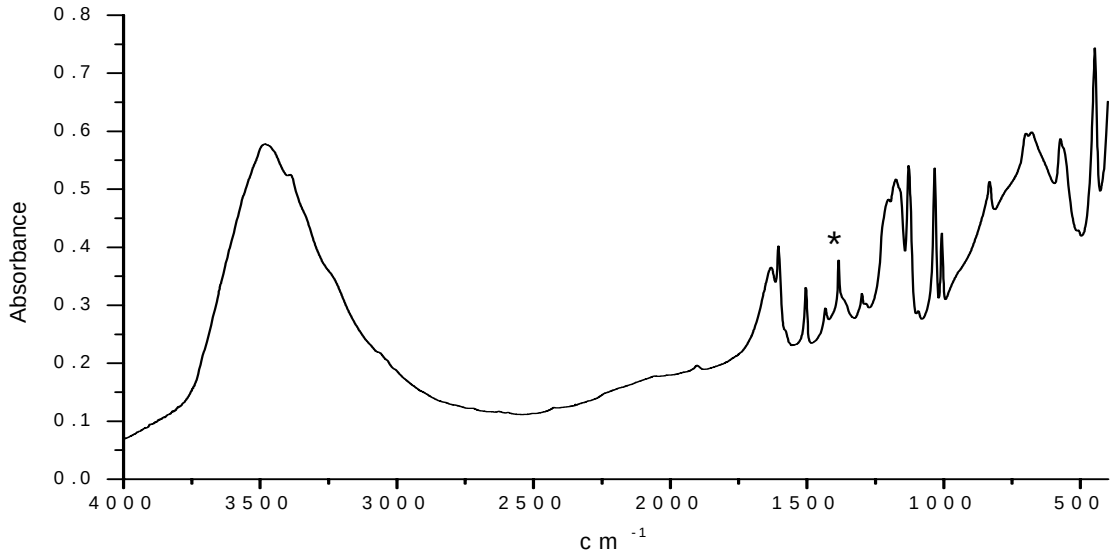

Figure 3.3: FTIR spectrum of 2:1 Mg-Al LDH sulfanilate. Residual nitrate is indicated by the asterisk*.

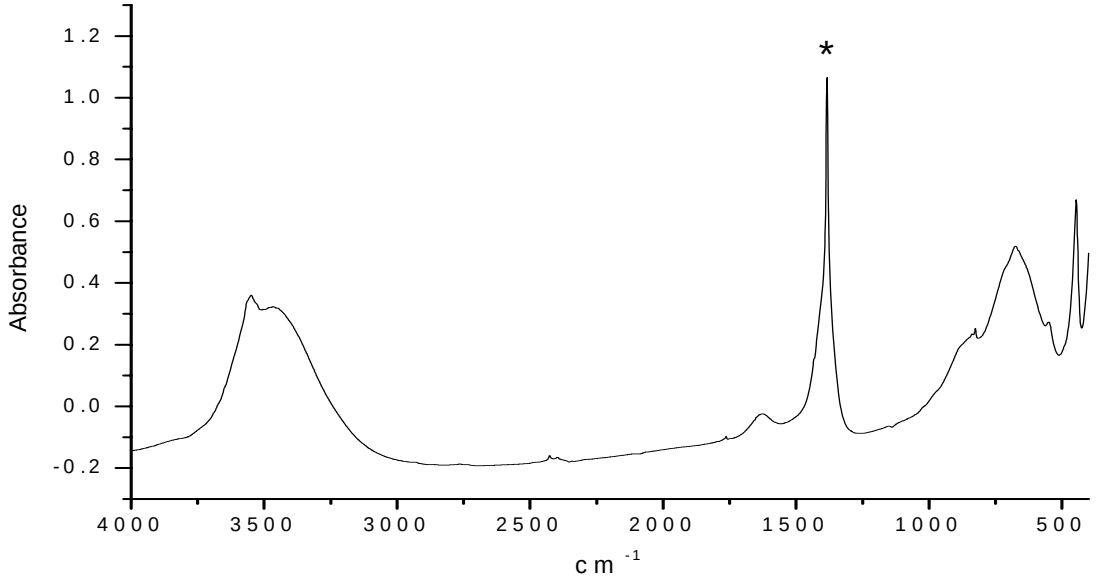

Figure 3.4: FTIR spectrum of aged 2:1 Mg-Al LDH NO_3. Nitrate peak is indicated by the asterisk*.

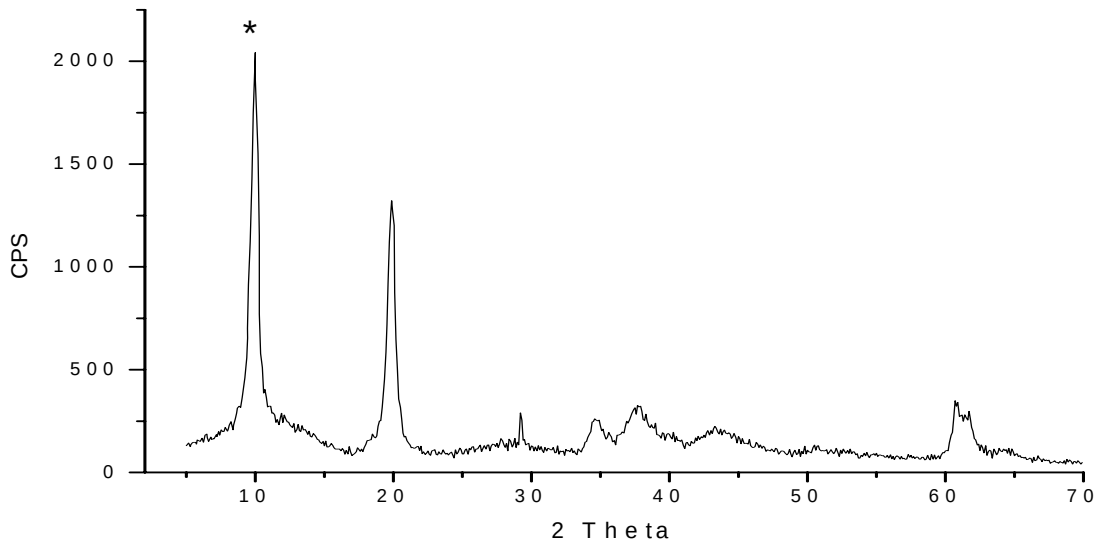

Figure 3.5: XRD pattern of aged 2:1 Mg-Al LDH NO_3. d_{003} is indicated by the asterisk*.

The XRD patterns of the Mg-Al LDH sulfanilate and Mg-Al sulfanilate with Ni are presented in Figures 3.6 and 3.8 and their similarity supports the assumption of minimal incorporation of nickel and also provides proof of no structural change in the LDH layers after nickel doping. The pattern for Mg-Al sulfanilate has a d_{003} of 16.32 which corresponds well with the size of sulfanilate anion plus the layer width. The peaks in the nickel doped material at 11 and 22^0 2theta and the d-spacing of 7.7Å for peak at 11^0 2theta, which is also the angle for d_{006} of sulfanilate, indicate presence of chloride in the interlayer spacing. The intercalation of chloride form the nickel chloride exchange could have caused this change. The decrease in the intensity of the d_{003} peak of sulfanilate around 5^0 2theta can also be explained by this assumption. The complete list of d-spacings with tentative assignments is given in Table 3.3 the atomic absorption spectroscopy data in Table 3.2 shows that there is very small amount incorporation of nickel in the material after doping and the ratio of the Mg to Al in this material remained close to 2. The

elemental analysis data presented in Table 3.2 shows that the experimental values for %C,%H,%N and %S are less than the theoretical values . This can be due to the incomplete exchange of nitrate in the precursor for the sulfanilate.

The comparisons of TGA and DTGA carried out in both air and nitrogen, presented in Figures 3.9 and 3.10 respectively show some significant change in the thermal behavior of the materials with and without nickel doping. The 2:1 Mg-Al LDH sulfanilate containing nickel needed higher temperatures for the first two weight loss steps but the final step occurs at slightly lower temperature for it than for the parent material this may be due to the difference in the interlayer composition i.e. presence of chloride in the material with nickel. The final %weight losses for both the materials in nitrogen are not very different from each other, the numbers being 46.17 and 48.10 for materials without and with nickel doping respectively and final residues after heat treatment are dark black in color for both the materials which can be interpreted as the color of the carbonaceous residue left. They show about same %weight losses in air also with 50.53% weight loss for material with nickel and with 49.58% for nickel doped material. The %weights of the Mg and al oxides which are the possible residues left after thermal decomposition are 55.5 and 56% for materials without and with nickel and these values agree well with the experimental %weight losses. The residue collected after TGA measurement for material without nickel in air is light brown, due may be to presence of some char along with the metal oxides and the nickel doped sample retains its pale green color which is color of nickel oxide which may be present along with aluminum and magnesium oxides. The weight loss steps seem to be requiring slightly lesser temperature in air than in nitrogen for both the materials.

Table 3.3 XRD data of 2:1 Mg-Al LDH sulfanilate with and without nickel.

2:1 Mg-Al LDH sulfanilate	(003)	(006)	(009)	(0012/0015)	(110/113)
Angle	5.65	10.99	19.30	35.05	60.89
d-spacing	15.63	8.04	4.59	2.56	1.52
2:1 Mg-Al LDH sulfanilate with Ni:	(003)	(003 of Cl)	(006 of Cl)	(0012 of Cl)	(110/113)
Angle	5.70	11.35	22.99	34.95	60.75
d-spacing	15.48	7.78	3.86	2.56	1.52

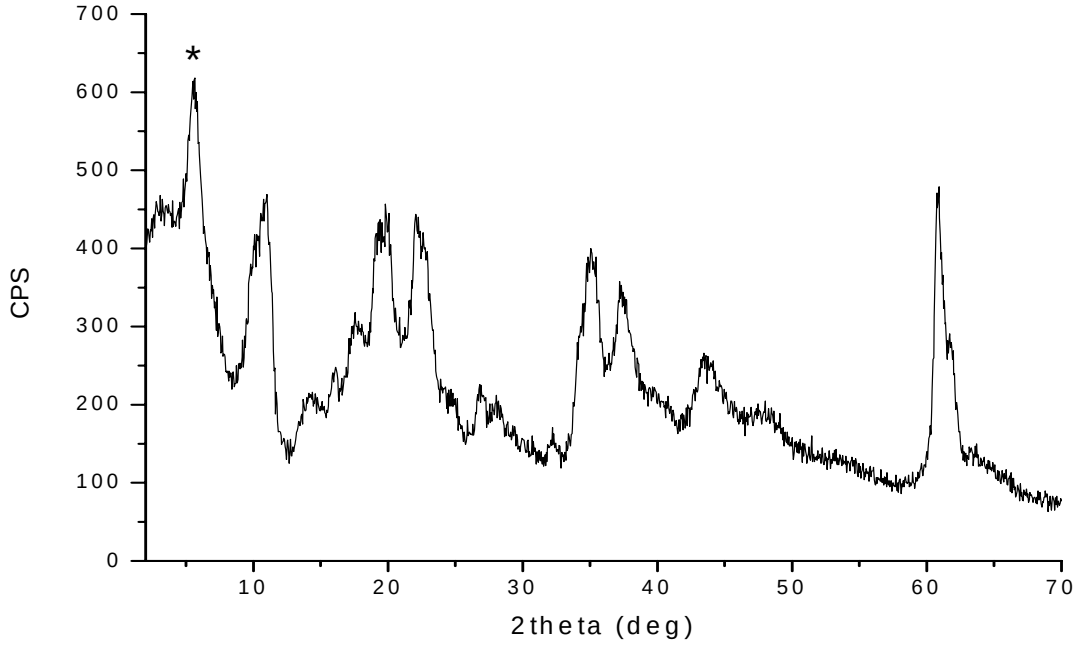

Figure 3.6: XRD pattern of 2:1 Mg-Al LDH sulfanilate. d_{003} is indicated by the asterisk*.

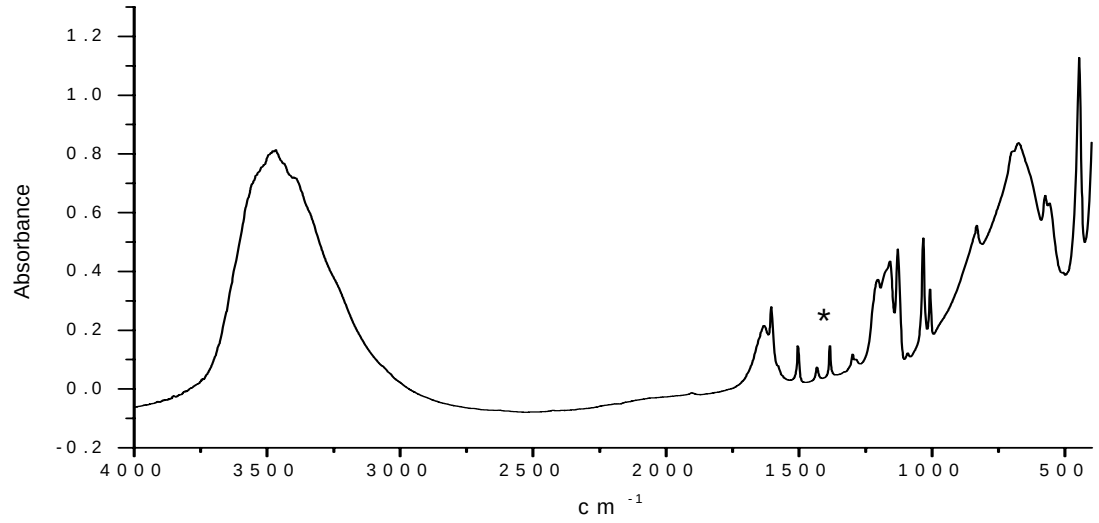

Figure 3.7: FTIR spectrum of 2:1 Mg-Al sulfanilate with nickel. Residual nitrate is indicated by the asterisk*.

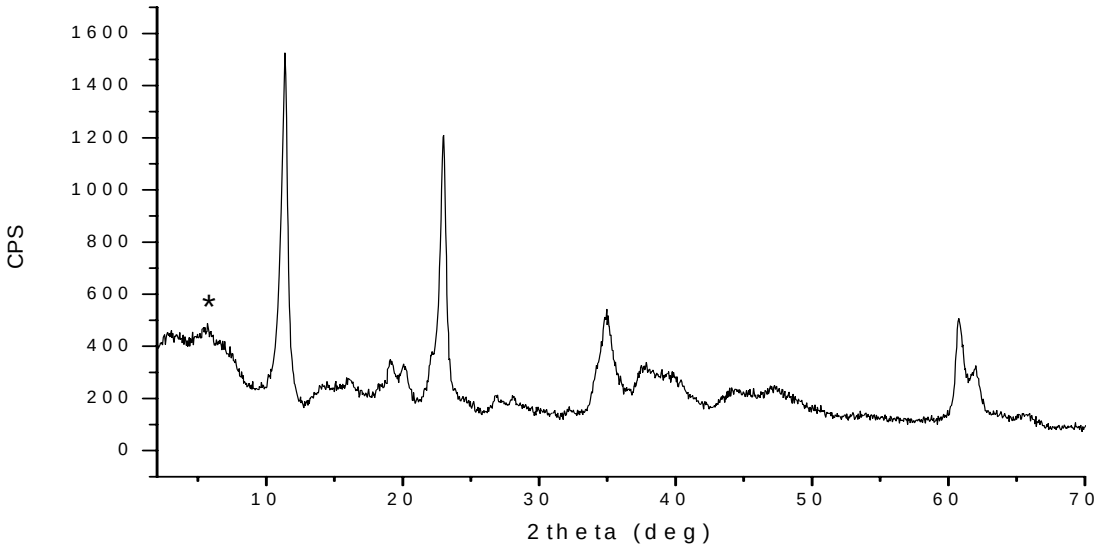

Figure 3.8: XRD pattern of 2:1 Mg-Al LDH sulfanilate with nickel. d_{003} is indicated by the asterisk*.

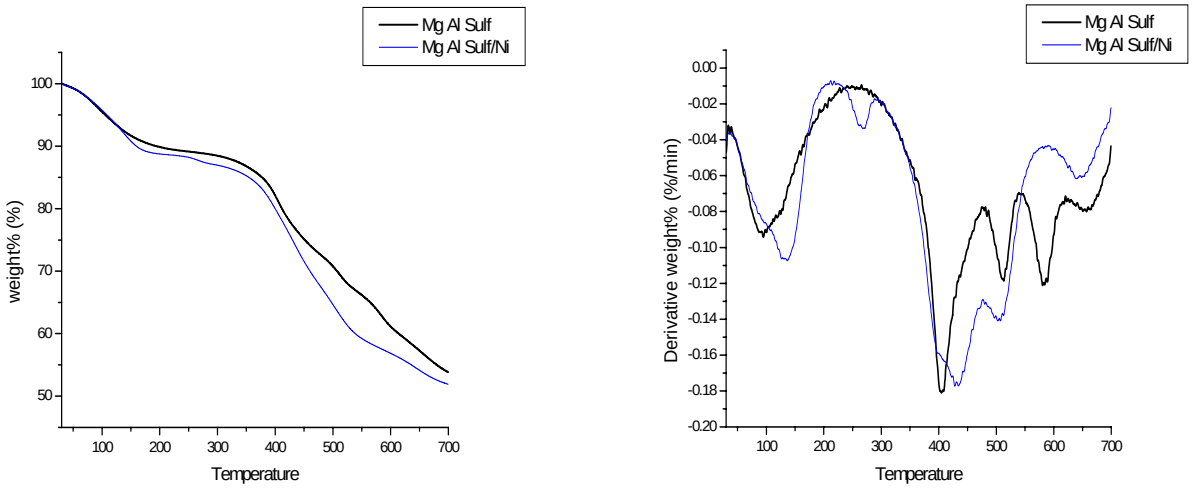

(a) (b)

Figure 3.9: (a) TGA comparison of 2:1 Mg-Al LDH sulfanilate with and without nickel in nitrogen. (b) DTGA comparison of 2:1 Mg-Al LDH sulfanilate with and without nickel in nitrogen.

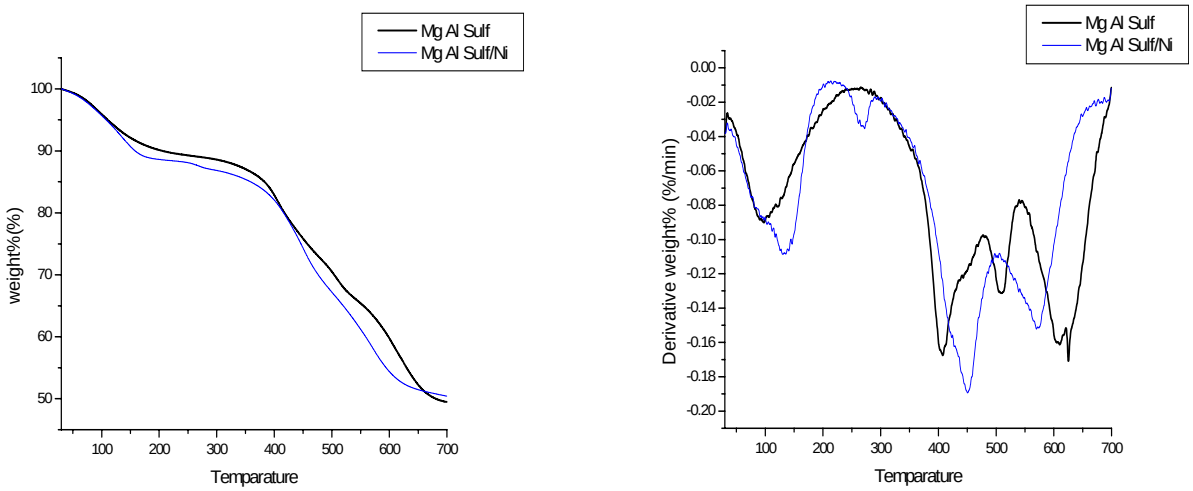

(a) (b)

Figure 3.10: (a) TGA comparison of 2:1 Mg-Al LDH sulfanilate with and without nickel in air. (b) DTGA comparison of 2:1 Mg-Al LDH sulfanilate with and without nickel in air.

b. 2:1 Zn-Al LDH Sulfanilate

In the case of 2:1 Zn-Al LDH nitrate also a 2:1 ratio of sulfanilate to nitrate was needed to get a nearly complete exchange. The peak around 425 cm^{-1} in the infrared spectrum in Figure 3.11 confirms the presence of 2:1 Zn-Al LDH. The infrared spectrum of nitrate precursor for this exchange is given in Figure 3.13.There was almost complete exchange of nitrate for sulfanilate. The residual nitrate peak around 1384cm^{-1}, indicated by asterisk in the spectrum is very small.

The 2:1 Zn-Al LDH sulfanilate was also doped with nickel and the analytical data of both the parent and the nickel doped LDH were compared. The infrared spectra in Figures 3.11 and 3.12 show no significant differences. The XRD patterns in the Figures 3.15 and 3.16 of the materials are also not different in their d_{003} values with the values being 15.61 and 15.56 for material without and with nickel respectively and this is an increase from the d-spacing of 8.85 for the nitrate precursor whose XRD pattern is given in Figure 3.14. The complete peak assignments for the XRD patterns for both the materials are given in the Table 3.5 and they show no significant differences. This, when coupled with the fact that the atomic absorption data shown in the Table 3.4 indicate the presence of nickel, leads us to believe that the nickel present is adsorbed on to the surface of the LDH layer and is neither in the gallery space nor 'in' the LDH sheets. The amount of nickel uptake however is very small and the ratio of Zn to Al in the Ni doped materials is also 2:1. The elemental analysis data is also presented in the Table 3.4 and the theoretical values for %C, %N, %H and %S are close to the experimental values.

Table 3.4 Atomic absorption spectroscopic results and elemental analysis data for 2:1 Zn-Al LDH sulfanilate with and without nickel (for the elemental analysis, T stands for theoretical and E stands for experimental).

LDH Sample	**%Zn**	**%Al**	**%Ni**	**Zn : Al**	**Zn : Ni**	**(Zn+Ni):Al**
Zn-Al Sulf	26.7	5.8	-	1.9:1	-	1.9:1
Zn-Al Sulf- Ni	27.9	5.7	1.0	2.0:1	23.6:1	2.0:1

LDH Sample	**%N_T**	**%N_E**	**%C_T**	**%C_E**	**%H_T**	**%H_E**	**%S_T**	**%S_E**
Zn-Al Sulf	2.99	3.16	15.39	15.48	3.44	3.38	6.85	7.04
Zn-Al Sulf-Ni	2.98	2.76	15.33	14.42	3.43	3.41	6.83	6.50

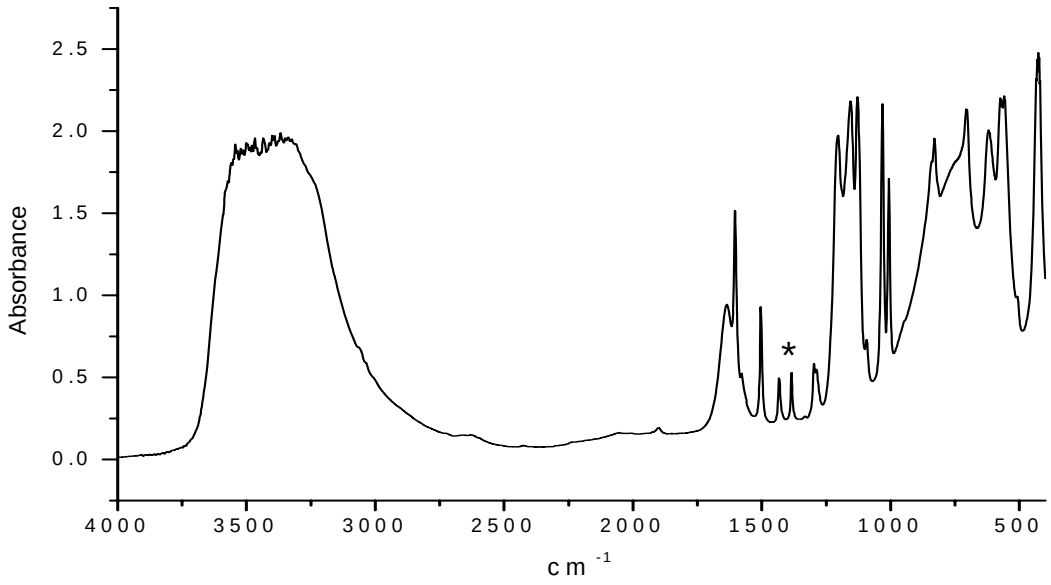

Figure 3.11: FTIR spectrum of 2:1 Zn-Al LDH sulfanilate. Residual nitrate is indicated by the asterisk*.

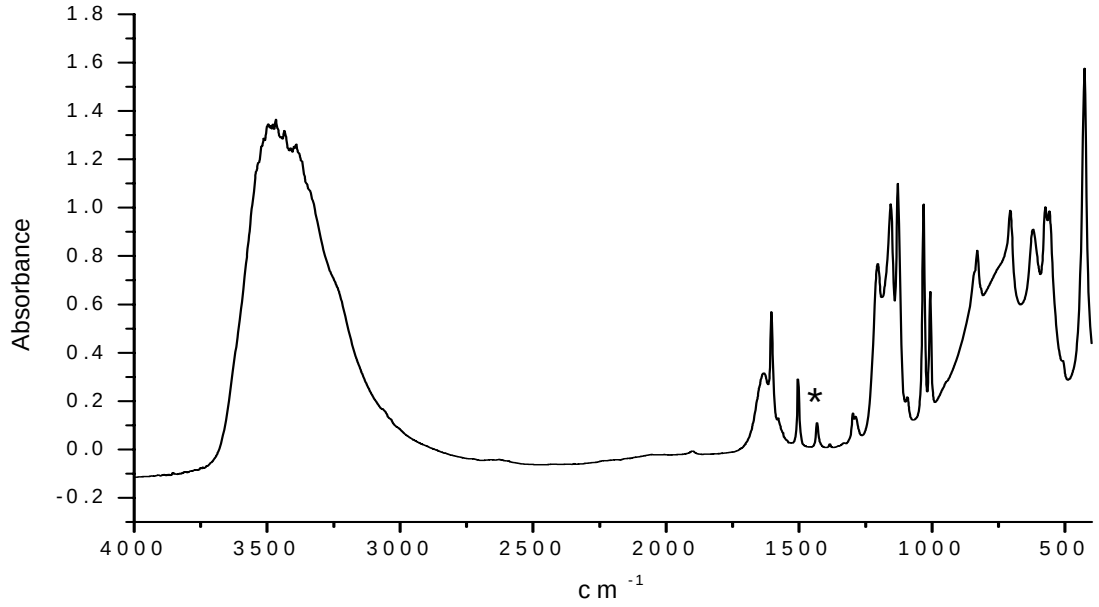

Figure 3.12: FTIR spectrum of 2:1 Zn-Al sulfanilate with nickel. Residual nitrate is indicated by the asterisk*.

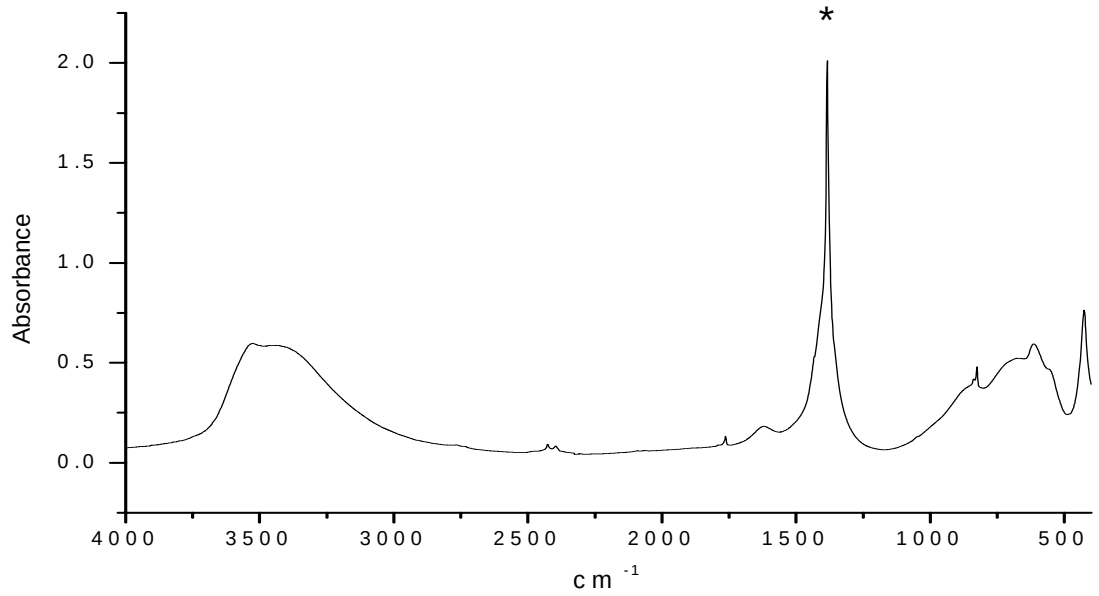

Figure 3.13: FTIR spectrum of aged 2:1 Zn-Al LDH NO_3. Nitrate peak is indicated by the asterisk*.

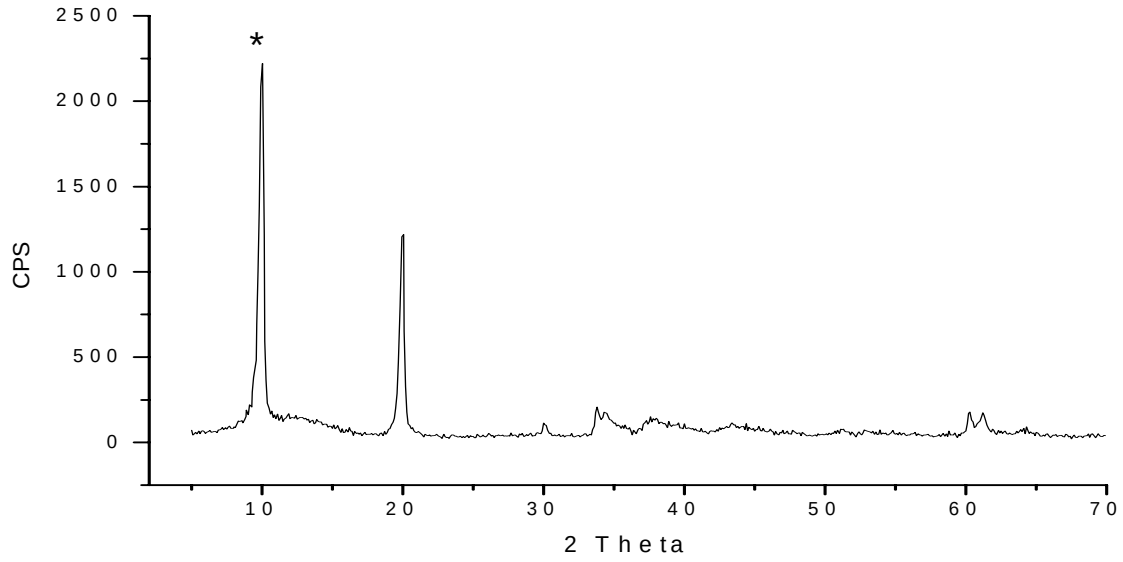

Figure 3.14: XRD pattern of aged 2:1 Zn-Al LDH NO_3. d_{003} is indicated by the asterisk*.

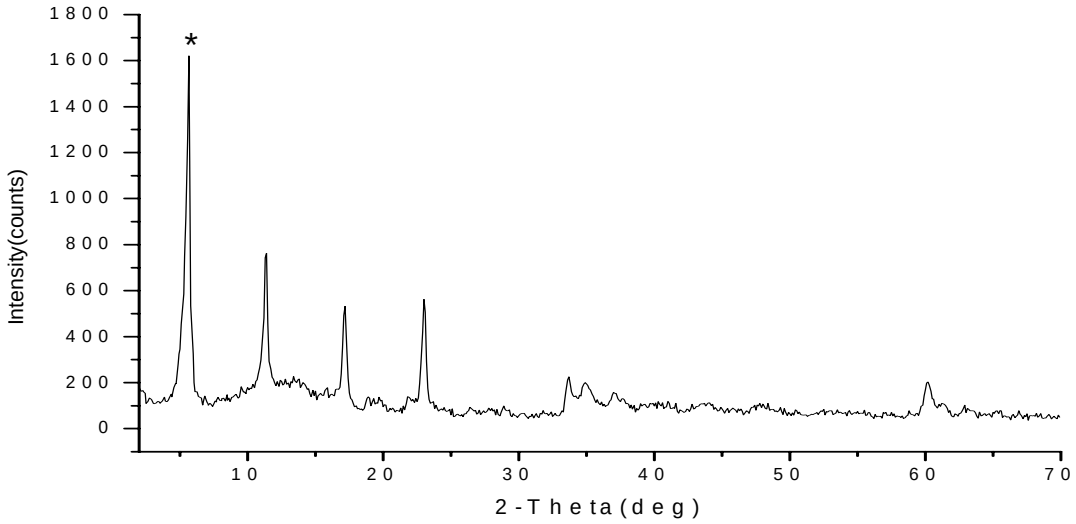

Figure 3.15: XRD pattern of 2:1 Zn-Al LDH sulfanilate.d_{003} is indicate by the asterisk*.

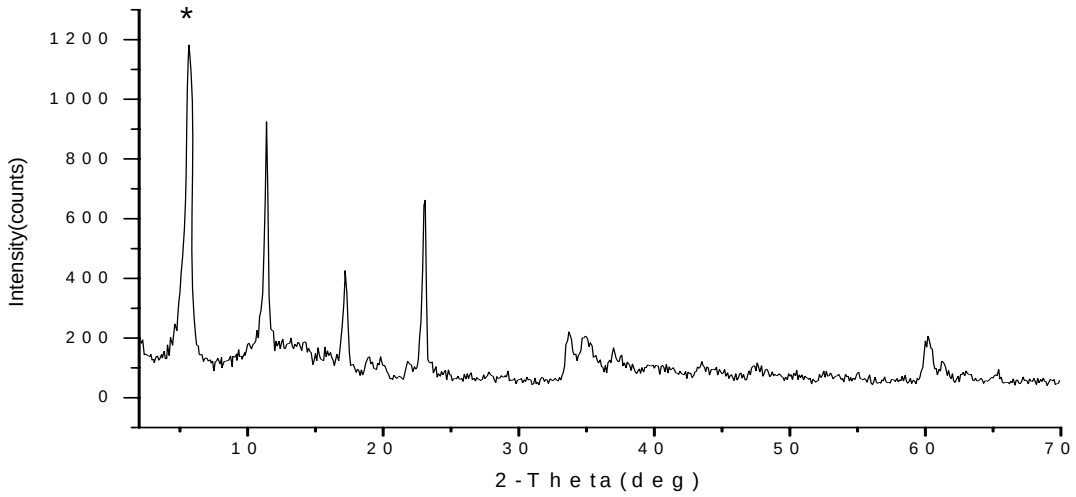

Figure 3.16 XRD pattern of 2:1 Zn-Al LDH sulfanilate with nickel.d_{003} is indicated by the asterisk*.

Table 3.5 XRD data for 2:1 Zn-l LDH sulfanilate with and without nickel.

2:1 Zn-l LDH sulfanilate	(003)	(006)	(009)	(0012)	(0015)	(015)	(110/ 113)
Angle	5.65	11.39	17.20	23.08	33.78	35.39	60.28
d-spacing	15.61	7.76	5.15	3.85	2.65	2.53	1.53
2:1 Zn-l LDH sulfanilate with Ni:	(003)	(006)	(009)	(0012)	(0015)	(015)	(110/ 113)
Angle	5.67	11.41	17.22	23.08	33.79	34.99	60.21
d-spacing	15.56	7.74	5.14	3.85	2.65	2.56	1.53

The comparisons TGA and DTGA of these materials collected in atmospheres of nitrogen and air are given in Figures 3.17 and 3.18 respectively and they show some differences. Again, this data show that the nickel doped material undergoes slower thermal degradation in nitrogen compared to the parent material, but perhaps slightly slower degradation in air. The residues after thermal treatment in nitrogen for both the materials were dark black, the color of carbonaceous

char which may be the product and the %weight losses are 42.92 and 42.61 for material with nickel and without nickel respectively. This agrees well with the theoretical residual weight of about 46% if Zn and Al oxides are to remain after the thermal degradation. The residues in the case of TGA in air retained their colors, i.e. white for the sample without nickel, indicating that the residue is a mixture of Al and Mg oxides and green for the one with nickel, the color of nickel oxide mixed with Al and Mg oxides and their % weight losses were 52.61 and 52.12. These values agree with the theoretical residual weight of oxides of Zn and Al which is around 46%. Again there was no significant difference in %weight loss for the samples with and without nickel, which suggests that the degradation products in both the cases are same and presence of nickel only accelerates the degradation. The main weight loss steps as seen in the DTGA occurred at higher temperature in air than in nitrogen.

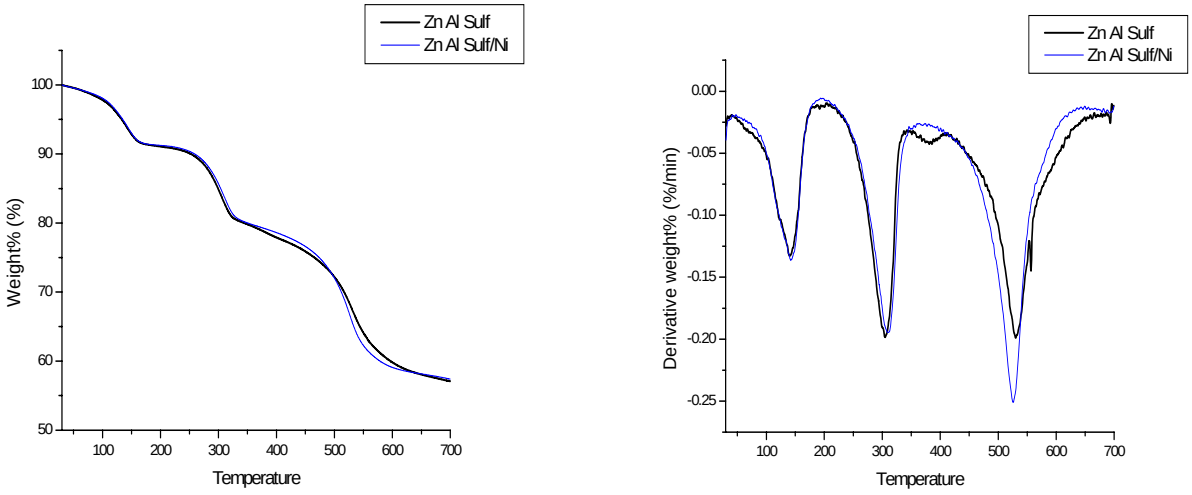

(a) (b)

Figure 3.17: (a) TGA comparison of 2:1 Zn-l LDH sulfanilate with and without nickel in nitrogen. (b) DTGA comparison of 2:1 Zn-l LDH sulfanilate with and without nickel in nitrogen.

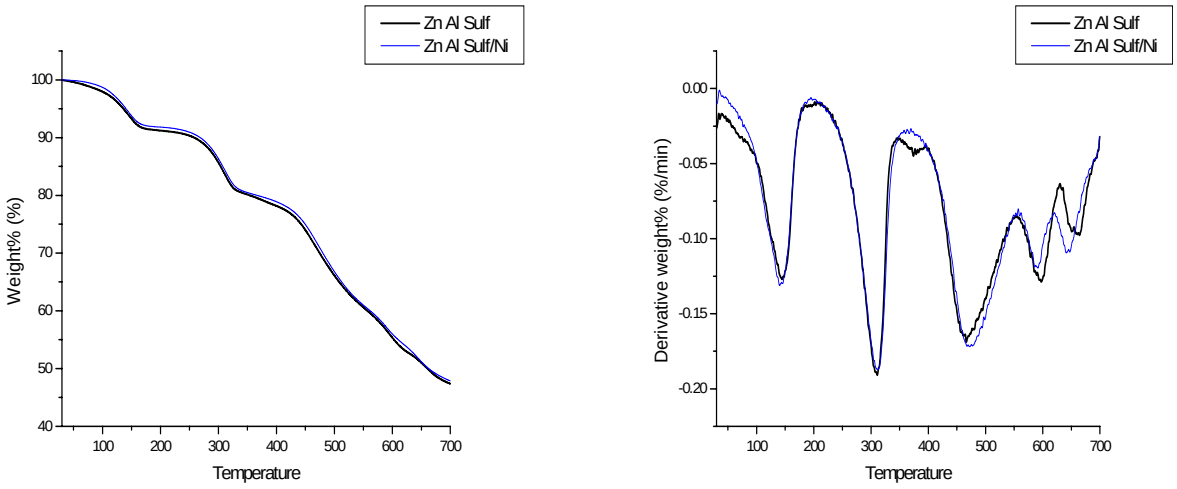

(a) (b)

Figure 3.18: (a) TGA comparison of 2:1 Zn-l LDH sulfanilate with and without nickel in air. (b) DTGA comparison of 2:1 Zn-l LDH sulfanilate with and without nickel in air.

3.4.2. *p*-Toluenesulfonate:

p-Toluenesulfonate was obtained by neutralizing *p*-toluenesulfonic acid obtained from the manufacturer with 50%w/w sodium hydroxide.

a. 2:1 Mg-Al LDH *p*-Toluenesulfonate:

Incorporation of *p*-toluenesulfonate into LDH was previously done and reported by other groups [6-9] and the reason for repeating is for the purpose of comparing its properties with the other anions studied and also the effects of nickel doping on thermal degradation of the material. The 2:1 Mg-Al LDH *p*-toluenesulfonate was prepared by exchanging the 2:1 Mg-Al LDH nitrate with one mole of *p*-toluenesulfonate for each mole of aluminum in the LDH nitrate. The infrared spectrum of sodium *p*-toluenesulfonate shown in Figures 3.19 shows sharp peaks at 1037 and 1176 cm^{-1}, for the symmetric and asymmetric S=O; sharp peaks at 1013, 1129 and 1497 cm^{-1} for

the aromatic CH groups and the aromatic C=C [8,9]. The infrared of 2:1 Mg-Al LDH *p*-toluenesulfonate in Figure 3.20 shows the peak around 444 cm^{-1} indicating the presence of 2:1 Mg-Al LDH. Comparing this spectrum with that of the nitrate precursor in Figure 3.4 reveals the decrease in the intensity of 1384cm^{-1} peak meaning the exchange has taken place.

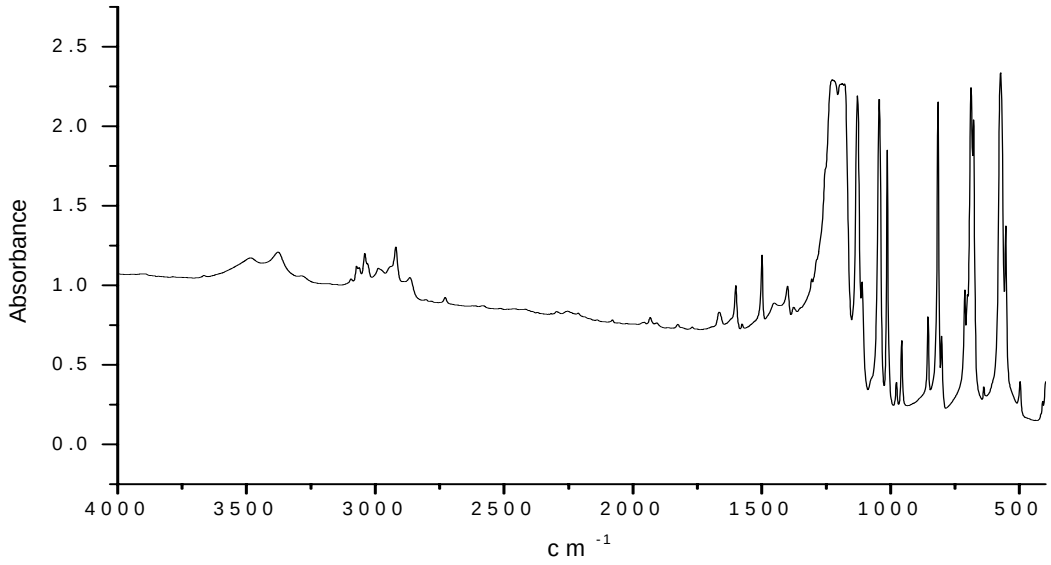

Figure3.19: FTIR spectrum of *p*-toluenesulfonate.

Table 3.6 XRD data for 2:1 Mg-Al LDH *p*-toluenesulfonate with and without nickel.

2:1 Mg-Al LDH *p*-toluenesulfonate	(003)	(006)	(009/0012)	(0015)	(0018)	(110/113)
Angle	4.99	10.28	20.59	25.70	34.78	60.89
d-spacing	17.66	8.59	4.31	3.46	2.57	1.52
2:1 Mg-Al LDH *p*-toluenesulfonate with Ni:	(003)	(006)	(009/0012)	(0015)	(0018)	(110/113)
Angle	4.99	10.31	20.60	25.62	34.69	60.97
d-spacing	17.67	8.57	4.30	3.47	2.58	1.51

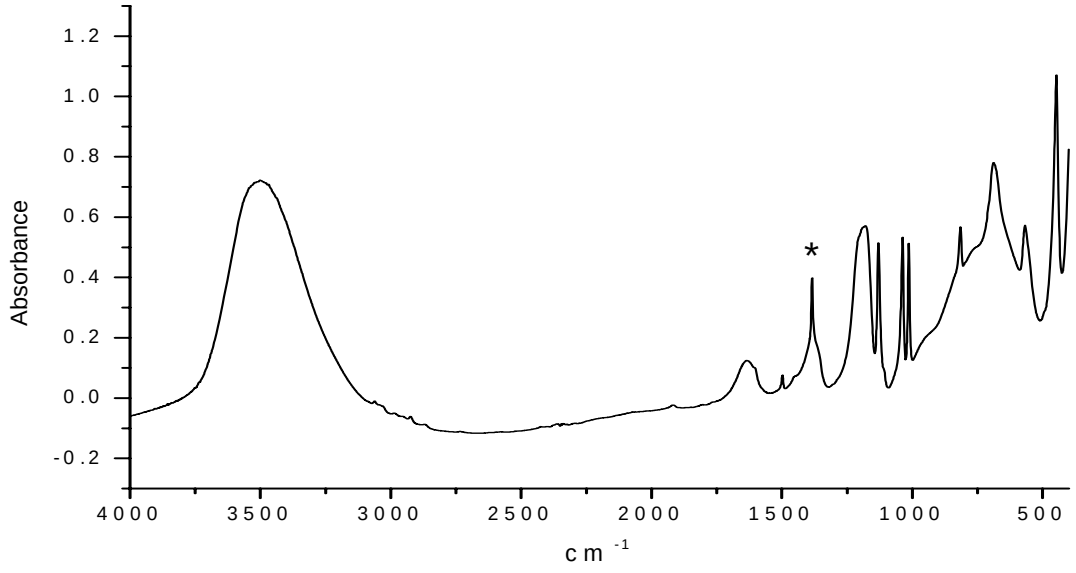

Figure 3.20: FTIR spectrum of 2:1 Mg-Al *p*-toluenesulfonate. Residual nitrate is indicated by the asterisk*.

The XRD pattern of 2:1 Mg-Al LDH *p*-toluenesulfonate in the Figure 3.21 gives proof of incorporation of *p*-toluenesulfonate into the interlayer space, its interlayer spacing has increased to 17.66 from 8.85 of XRD pattern of the nitrate precursor in Figure 3.5. The complete peak listings for the pattern are given in the Table 3.6.

Table 3.7 Atomic absorption spectroscopy results and elemental analysis data for 2:1 Mg-Al LDH *p*-toluenesulfonate with and without nickel.

LDH Sample	**%Mg**	**%Al**	**%Ni**	**Mg : Al**	**Mg : Ni**	**(Mg+Ni):Al**
Mg-Al PTS	12.1	6.7	0	2.0	-	2.0:1
Mg-Al PTS-Ni	12.5	6.6	4.6	2.1	6.6	2.3:1

LDH Sample	**%N_T**	**%N_E**	**%C_T**	**%C_E**	**%H_T**	**%H_E**	**%S_T**	**%S_E**
Mg-Al PTS	0.0	0.3	20.9	16.8	4.3	4.4	8.0	5.6
Mg-Al PTS-Ni	0.0	0.0	20.5	15.6	4.2	4.5	7.8	5.2

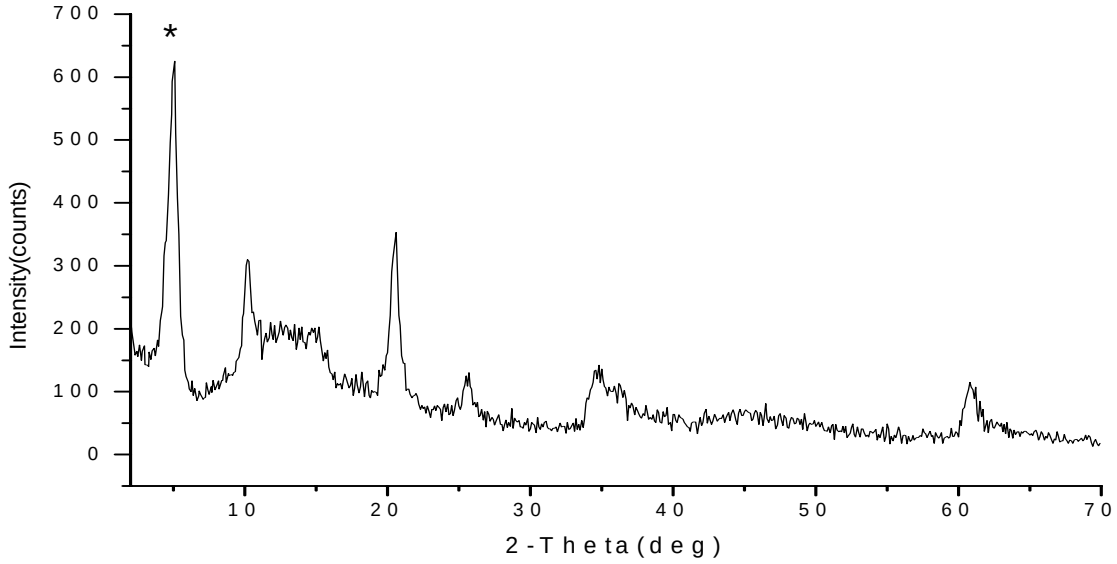

Figure 3.21: XRD pattern for 2:1 Mg-Al LDH *p*-toluenesulfonate. d_{003} is indicated by the asterisk*.

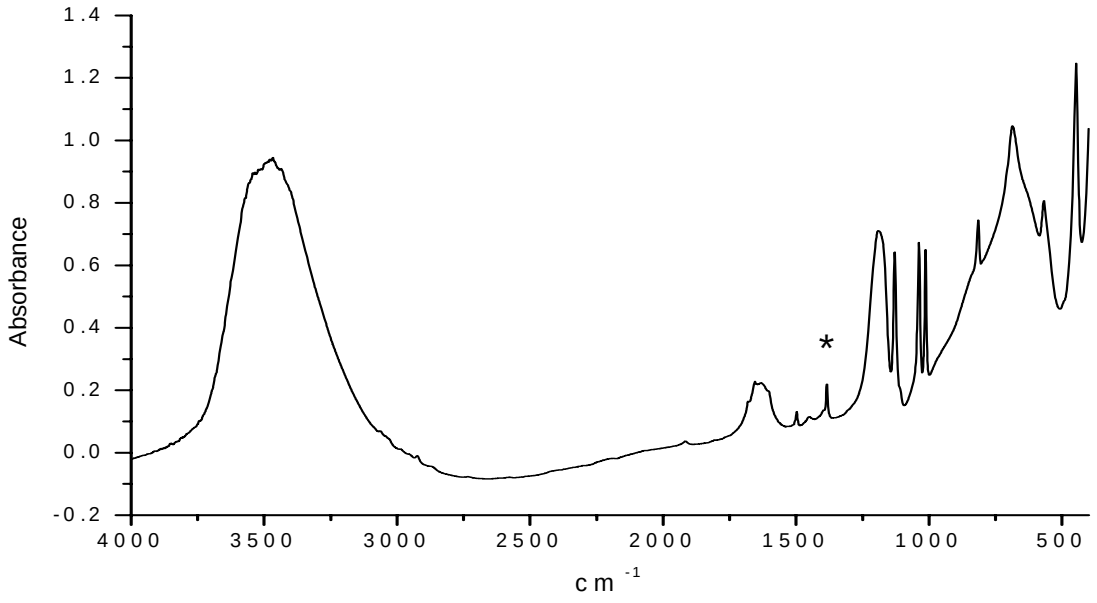

Figure 3.22: FTIR spectrum of 2:1 Mg-Al LDH *p*-toluenesulfonate with nickel. Residual nitrate is indicated by the asterisk*.

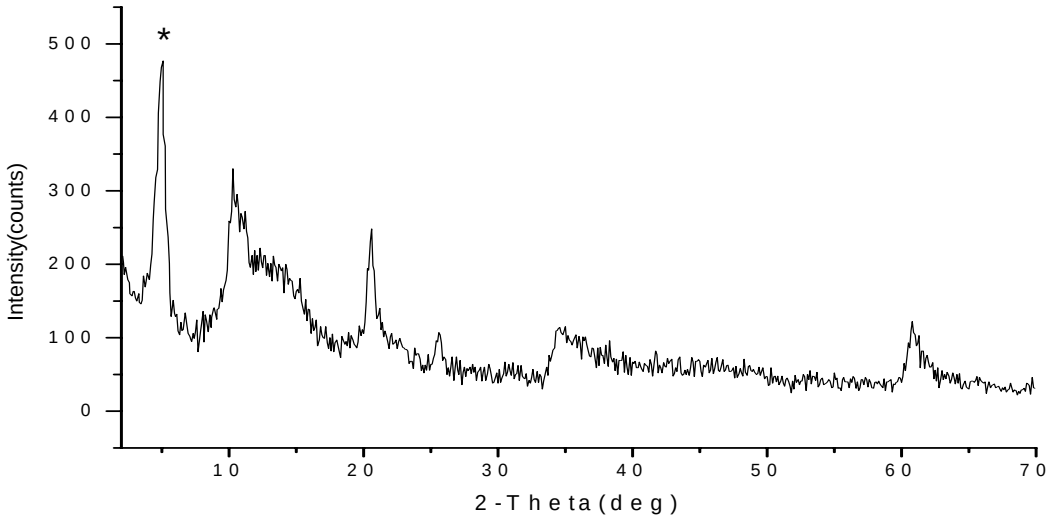

Figure 3.23: XRD pattern for 2:1 Mg-Al LDH *p*-toluenesulfonate with nickel. d_{003} is indicated by the asterisk*.

The material was also doped with nickel and was observed for any differences this incorporation would bring. The infrared and XRD patterns for the nickel doped material given in Figures 3.22 and 3.23 show no significant differences from those of the parent material. The d_{003} values for both the materials are 17.66 and 17.67. The presence of nickel however is proved by the green color of the product and the atomic absorption results given in the Table 3.7. The Mg-Al ratios are 2:1 for both the materials. The elemental analysis data given in the Table 3.7 show that the experimental percentages of C,H,N and S are less than the theoretical values which may be due to the incomplete exchange of nitrate for PTS. The 1384 cm^{-1} peaks, indicative of residual nitrate in the infrared so the materials in Figures 3.20 and 3.22 also support this idea.

The TGA and DTGA comparisons of the parent material and the nickel doped material in Figures 3.24 and 3.25 provide proof of difference between the materials. The thermal degradation of material with nickel is slower than that of the parent material in both nitrogen and

air. The residues after thermal treatment in nitrogen were dark black in color, which can be due to the carbonaceous char formed in the thermal process and the %weight losses were 43.37 and 48.06 for material without nickel and with nickel respectively. The %weight of Mg and Al oxides, which are theoretical residues formed in the thermal treatment of these substances are 58% and 56.5% and these values agree with the %weight loss found out experimentally. In air the material with nickel retained its green color, the color of nickel oxide residue and the one without nickel turned to light brown from its original white color after heating, due may be to presence of some char. The % weight losses in air were 51.5 and 54.5 for materials with and without nickel respectively and these values also agree with the theoretical weight% of residual Mg and Al oxides.

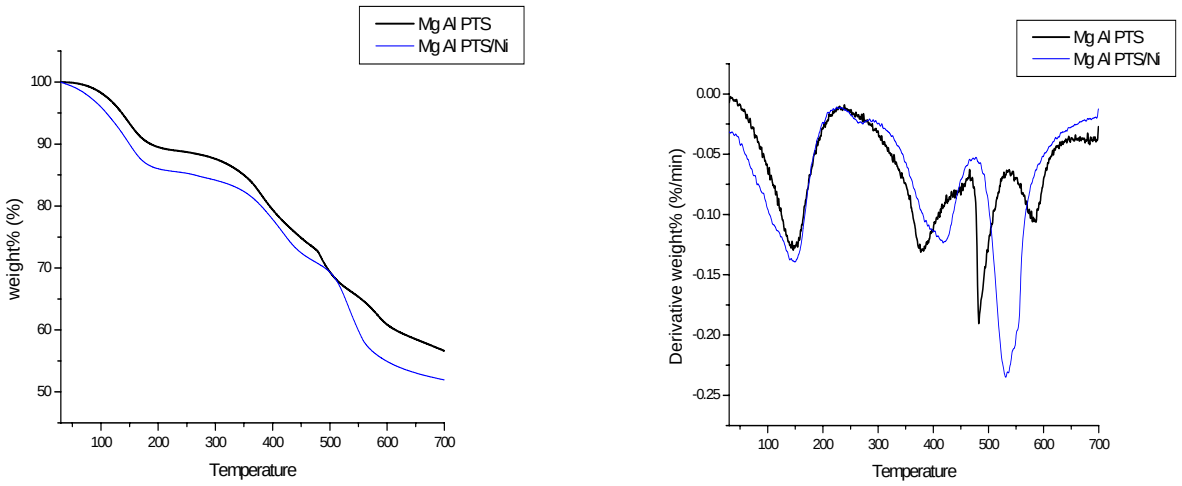

(a) (b)

Figure 3.24: (a) TGA comparison of 2:1 Mg-Al LDH *p*-toluenesulfonate with and without nickel in nitrogen. (b) DTGA comparison of 2:1 Mg-Al LDH *p*-toluenesulfonate with and without nickel in nitrogen.

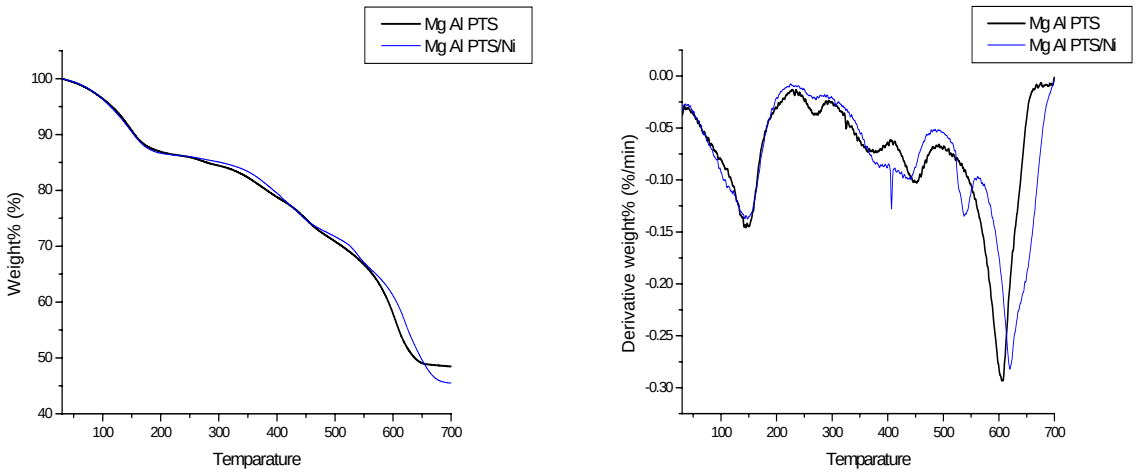

.

(a) (b)

Figure 3.25: (a) TGA comparison of 2:1 Mg-Al LDH *p*-toluenesulfonate with and without nickel in air. (b) DTGA comparison of 2:1 Mg-Al LDH *p*-toluenesulfonate with and without nickel in air.

b. 2:1 Zn-Al LDH *p*-Toluenesulfonate:

In this case also one mole of *p*-toluenesulfonate per each mole of aluminum in the LDH was enough to get a nearly complete exchange with the nitrate in the precursor. The infrared spectrum of the 2:1 Zn-Al LDH *p*-toluenesulfonate in Figure 3.26 shows evidence of 2:1 Zn-Al LDH and the almost complete exchange of nitrate with *p*-toluenesulfonate i.e. it contains the peak at 425 cm^{-1} peak and also shows a very short 1384 cm^{-1} peak.

The XRD of the material in the Figure 3.28 with a d_{003} of 17.68 illustrates presence of *p*-toluene sulfonate in the interlayer space, this is increase from a d_{003} of 8.85 of the XRD pattern of the of nitrate precursor in Figure 3.14. A complete list of tentative d-spacings is given in the Table 3.9.

This parent material also when doped with nickel shows no structural changes and this can be demonstrated by the similarity of its infrared and XRD patterns in Figures 3.27 and 3.29

with those of the parent material. However, again the atomic absorption results of the material when compared to that of the parent as in Table 3.8 provide evidence of the nickel in the sample. The 2:1 ratio between Zn and Al however is maintained even in the nickel doped material because of incorporation of very small amount of nickel. The elemental analysis data which is also presented in the Table 3.8 shows that the experimental values for %C, %H, %N and %S are close to the theoretical values.

The TGA and DTGA comparisons of the parent and the nickel doped material in the Figures 3.30 and 3.31 also differ in that the thermal degradation of nickel doped material is faster than that of the parent compound and the last endothermic peak in the DTGAs of the materials to be occurring at lower temperature in nitrogen than in air. The residues after the TGA in nitrogen looked dark black, the color of carbonaceous char, the possible product, for both the materials, whereas in air the materials retained their colors i.e. white for the one without nickel and green for the one with nickel, the colors of the metal oxides present in them. The % weight losses for the materials with and with out nickel are 42.77 and 43.18 in nitrogen and 53.48 and 52.43 in air respectively. The %weight of the oxides of Zn and Al which are the possible residues after thermal treatment of these materials is around 48% and 47% and these figures agree well within a difference of about 5 units both in nitrogen and air. Presence of some carbonaceous char in the samples treated in nitrogen may be the reason for their lesser weight loss. Once again, the weight loss steps occurred at higher temperature in air than in nitrogen.

Table 3.8: Atomic absorption spectroscopy results and elemental analysis data for 2:1 Zn-Al LDH *p*-toluenesulfonate with and without nickel.

LDH Sample	**%Zn**	**%Al**	**%Ni**	**Zn : Al**	**Zn : Ni**	**(Zn+ Ni):Al**
Zn-Al PTS	26.9	5.6	0	2.1	-	2.1:1
Zn-Al PTS-Ni	26.9	5.6	0.7	2.0	32.5	2.0:1

LDH Sample	**%N_T**	**%N_E**	**%C_T**	**%C_E**	**%H_T**	**%H_E**	**%S_T**	**%S_E**
Zn-Al PTS	0.0	0.2	17.3	17.3	3.5	3.9	6.6	6.6
Zn-Al PTS-Ni	0.0	0.0	17.3	16.0	3.5	3.7	6.6	6.0

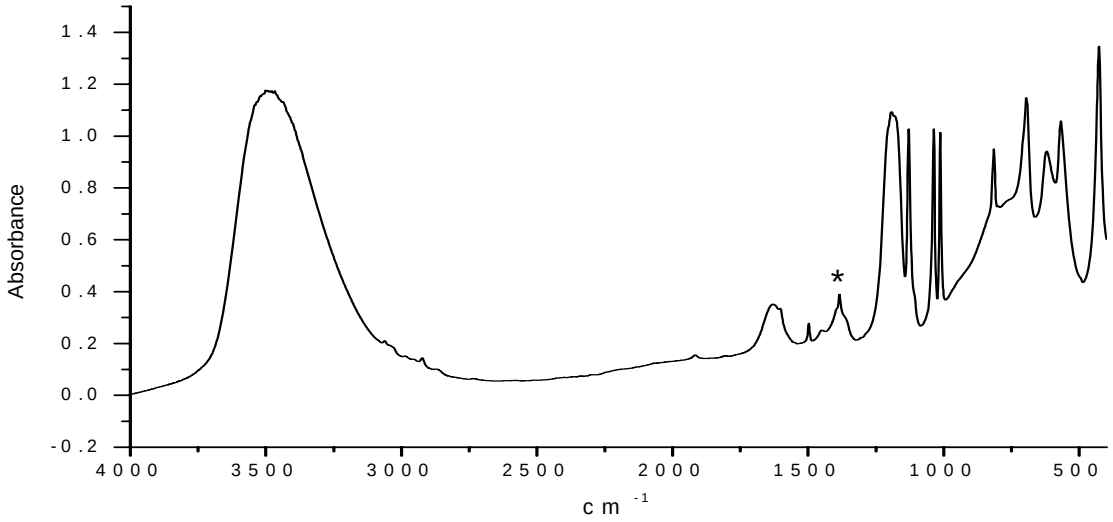

Figure 3.26: FTIR spectrum of 2:1 Zn-Al LDH *p*-toluenesulfonate. Residual nitrate is indicated by the asterisk*.

Table 3.9 XRD data for 2:1 Zn-Al LDH *p*-toluenesulfonate with and without nickel.

2:1 Zn-Al LDH *p*-toluenesulfonate	(003)	(006)	(009)	(0012)	(0015)	(015)	(110/ 113)
Angle	5.10	10.27	15.40	20.61	25.86	34.50	60.41
d-spacing	17.29	8.60	5.74	4.30	3.44	2.59	1.53
2:1 Zn-Al LDH *p*-toluenesulfonate with Ni:	(003)	(006)	(009)	(0012)	(0015)	(015)	(110/ 113)
Angle	4.99	10.19	15.29	20.52	25.70	33.89	60.36
d-spacing	17.67	8.67	5.78	4.32	3.46	2.64	1.53

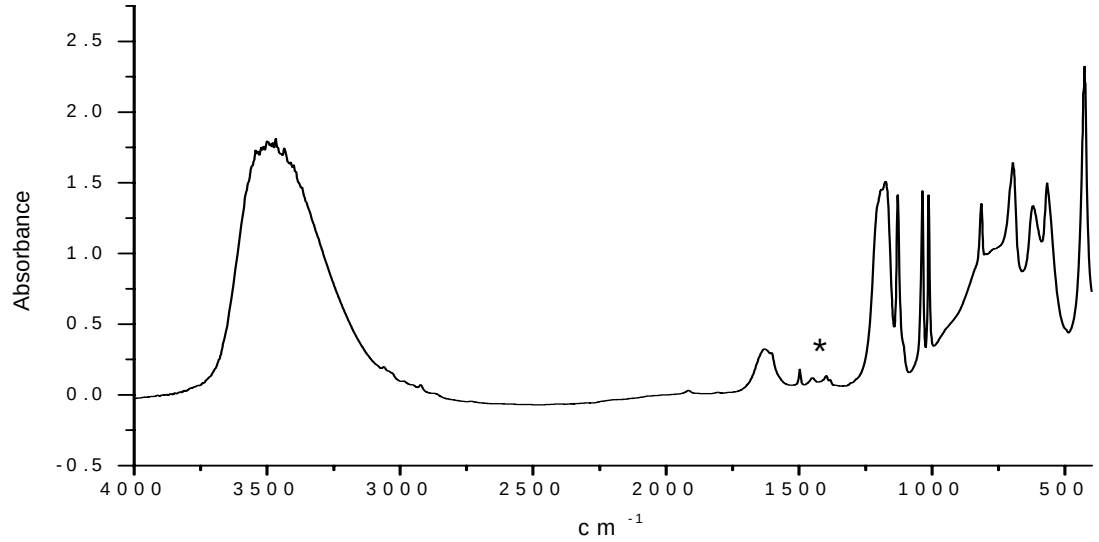

Figure 3.27: FTIR spectrum of 2:1 Zn-Al LDH *p*-toluenesulfonate with nickel. Residual nitrate is indicated by the asterisk*.

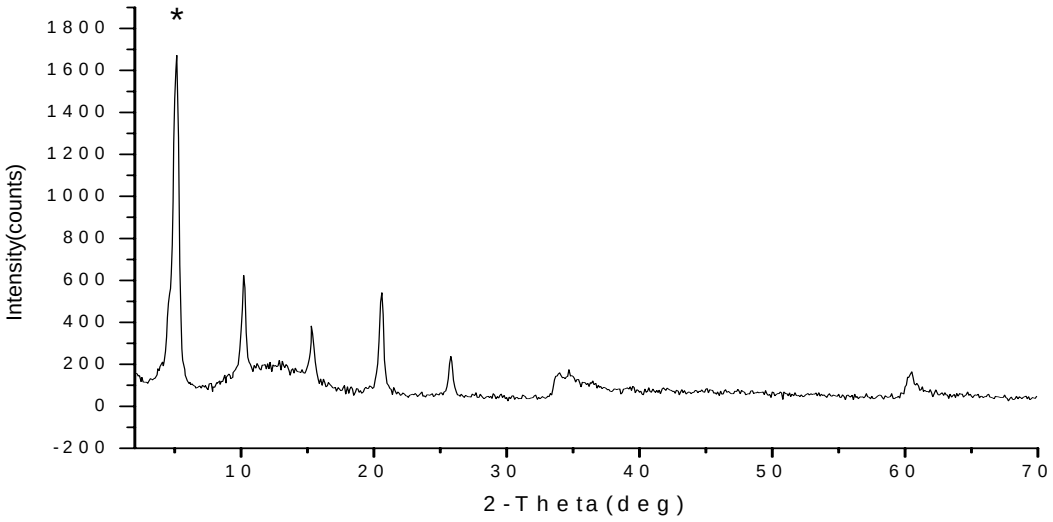

Figure 3.28: XRD pattern of 2:1 Zn-Al LDH *p*-toluenesulfonate. d_{003} is indicated by the asterisk*.

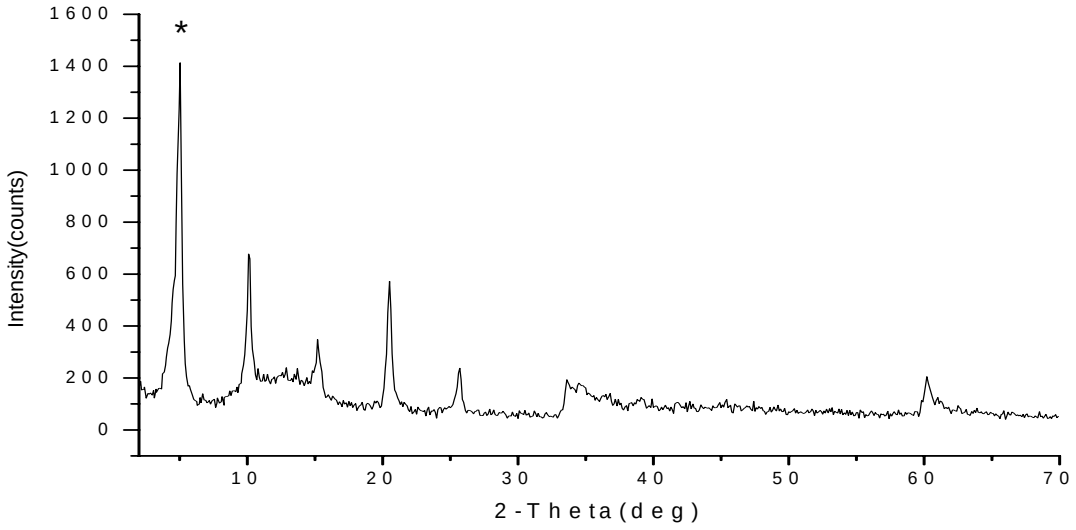

Figure 3.29: XRD pattern of 2:1 Zn-Al LDH *p*-toluenesulfonate with nickel. d_{003} is indicated by the asterisk*.

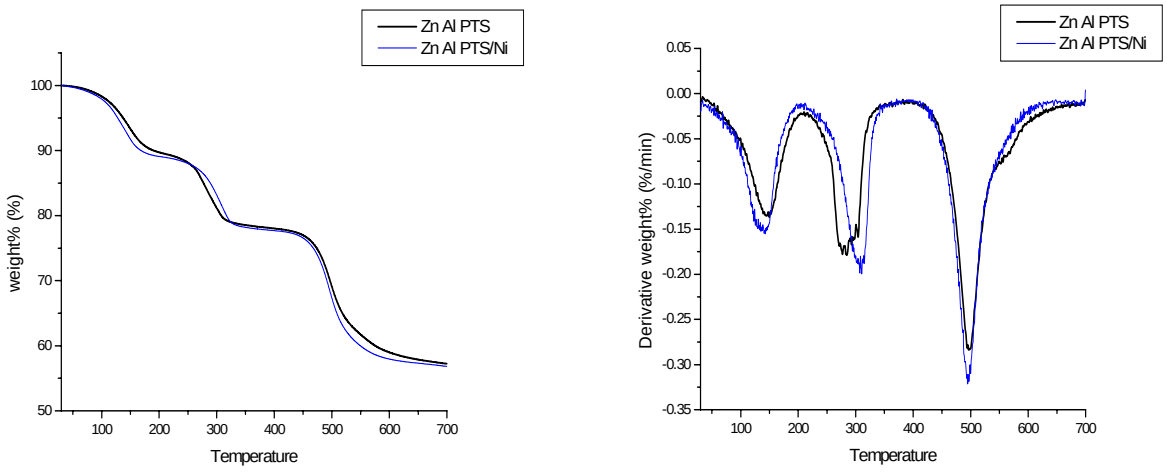

(a) (b)

Figure 3.30: (a) TGA comparison of 2:1 Zn-Al LDH *p*-toluenesulfonate with and without nickel in nitrogen. (b) DTGA comparison of 2:1 Zn-Al LDH *p*-toluenesulfonate with and without nickel in nitrogen.

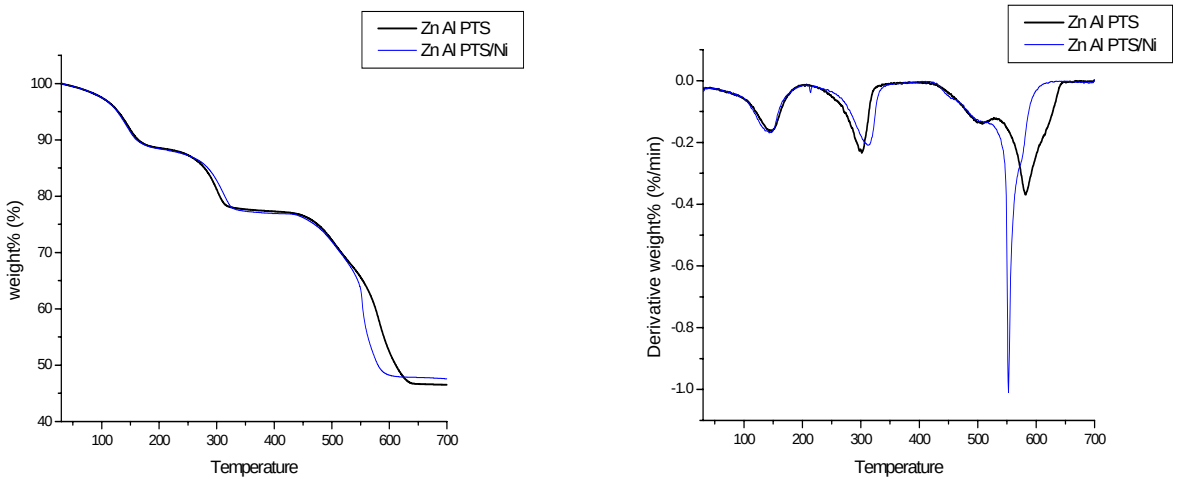

(a) (b)

Figure 3.31: (a) TGA comparison of 2:1 Zn-Al LDH *p*-toluenesulfonate with and without nickel in air. (b) DTGA comparison of 2:1 Zn-Al LDH *p*-toluenesulfonate with and without nickel in air.

3.4.3. 4-Chlorobenzenesulfonate

The 4-chlorobenzenesulfonate was prepared by neutralizing 4-chlorobenzenesulfonic acid obtained from the manufacturer with 50%w/w sodium hydroxide.

a. 2:1 Mg-Al LDH 4-Chlorobenzenesulfonate

4-chlorobenzenesulfonate intercalated Zn Al LDH was recently reported[10] and in this study the Mg Al LDH 4-chlorobenzensulfonate preparation and nickel doping were also carried out. One mole of 4-chlorobenzenesulfonic acid per each mole of aluminum in the LDH was sufficient to get a nearly complete exchange with the nitrate in the precursor as in the case of *p*-toluenesulfonate. The infrared spectrum of pure 4-chlorobenzenesulfonic acid is given in the Figure 3.32 and it shows sharp peaks at 1030, 1185 and 1230 cm^{-1}, for the symmetric and asymmetric S=O; sharp peaks at 1010, 1130 and 1480 cm^{-1} for the aromatic CH groups and the

aromatic C=C) [12]. The infrared spectrum of 2:1 Mg-Al LDH 4-chlorobenzenesulfonate in the Figure 3.33 has the evidence of presence of 2:1 Mg-Al LDH in that it has the 444 cm^{-1} and also the reduction in the peak at 1384 cm^{-1} from the infrared of the nitrate precursor given in the Figure 3.4 demonstrates the exchange of nitrate in the precursor for 4-chlorobenzenesulfonate.

Table 3.10 Atomic absorption spectroscopy and elemental analysis data for 2:1 Mg-Al LDH 4-chlorobenzenesulfonate with and without nickel.

LDH Sample	**%Mg**	**%Al**	**%Ni**	**Mg : Al**	**Mg : Ni**	**(Mg+Ni):Al**
Mg-Al CBS	13.2	6.7	-	2.2 : 1	-	2.2:1
Mg-Al CBS-Ni	12.5	6.6	4.9	2.1 : 1	6.0 : 1	2.3:1

LDH Sample	**%N_T**	**%N_E**	**%C_T**	**%C_E**	**%H_T**	**%H_E**	**%S_T**	**%S_E**
Mg-Al CBS	0.00	0.43	17.68	12.61	3.48	3.50	7.91	6.94
Mg-Al CBS-Ni	0.00	0.02	17.51	11.07	3.42	3.48	7.79	6.24

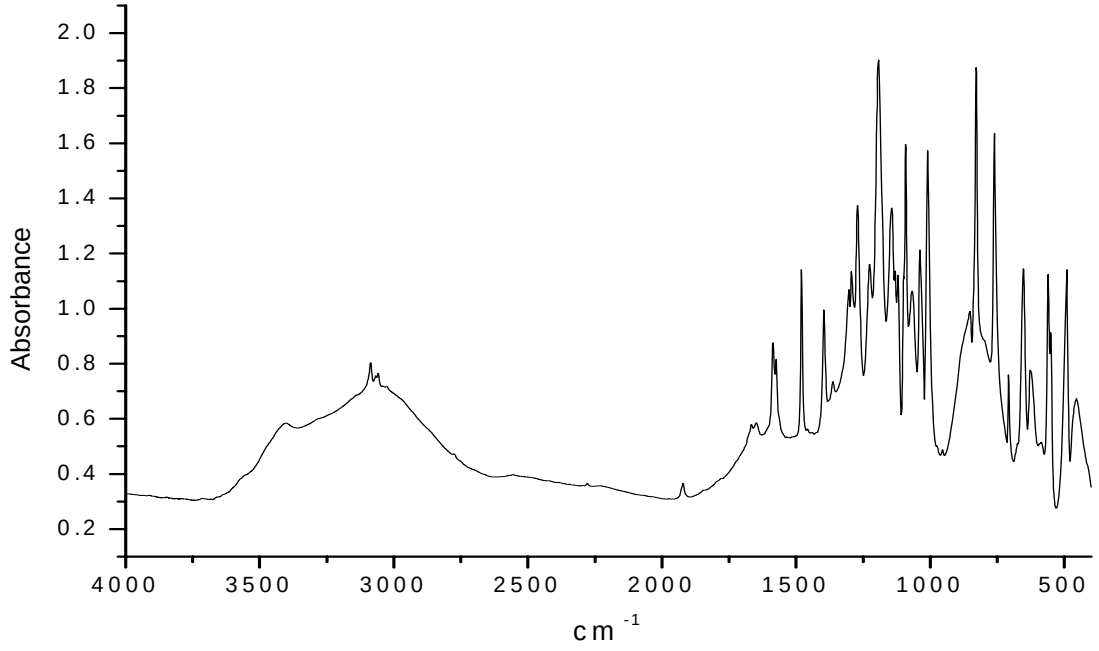

Figure 3.32: FTIR spectrum of sodium 4-chlorobenzenesulfonate.

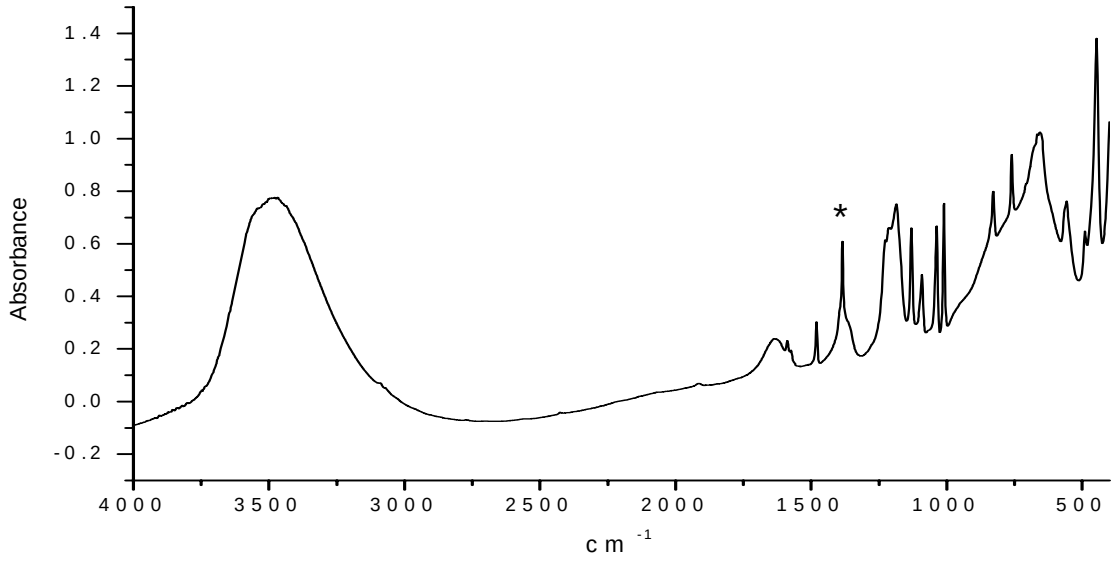

Figure 3.33: FTIR spectrum of 2:1 Mg-Al LDH 4-chlorobenzenesulfonate. Residual nitrate is indicated by the asterisk*.

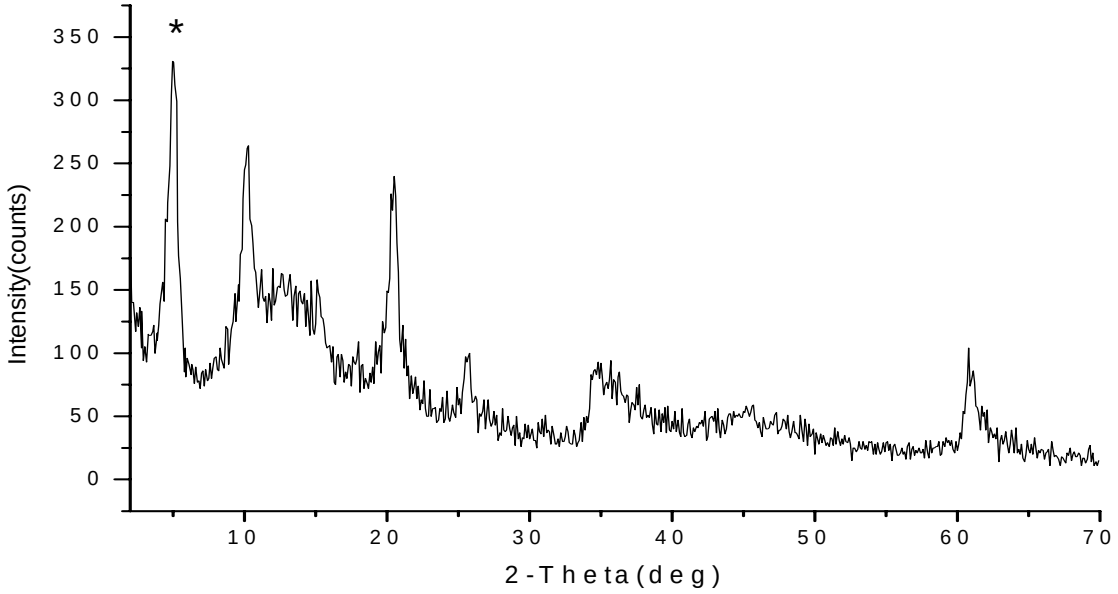

Figure 3.34: XRD pattern of 2:1 Mg-Al LDH 4-chlorobenzenesulfonate. d_{003} is indicated by the asterisk*.

The XRD pattern of the material in the Figure 3.34 also shows the incorporation of 4-cholrobenzenesulfonate into the interlayer space. The d_{003} value, which is the measure of

interlayer spacing of the LDH, had increased from 8.85 in nitrate precursor in Figure 3.5 to 17.35 in Figure 3.35. The complete list of tentative d-spacings is given in the Table 3.11.

This material also when doped with nickel, as the other materials discussed above does not show any structural changes. This can be illustrated by comparing the infrared spectrum and XRD pattern of this material in Figures 3.35 and 3.36 with its parent material. The d_{003} of the parent is 17.35 and is very similar to that of the material with nickel which is 17.15. The patterns however are slightly dissimilar in the appearance of peaks. The atomic absorption data in the Table 3.10 again give proof of the presence of nickel in the material. The ratio of Mg to Al remains close to 2 even after doping with nickel due to presence of a very small amount of nickel. The elemental analysis data, also given in Table 3.10, show that the experimental values for %C, %H, %N and %S are smaller than the theoretical values. This can also be explained by the fact that the exchange of nitrate for CBS was not complete.

The TGA and DTGA comparisons in nitrogen and air in Figures 3.37 and 3.38 of both the materials show that the thermal degradation of nickel doped material is faster than that of the parent material. The final residues of thermal treatment in nitrogen for both the materials again looked dark black in color and in air the material without nickel looked pale brown while the material with nickel retained its green color. The %weight losses for materials with and without nickel were 50.61 and 50.05 in nitrogen and 53.74 and 56.82 in air respectively. The theoretical %weight of Mg and Al oxides which are the possible residues is 58% and 57% and this agrees with the %weight losses obtained form the thermal analysis. The weight loss steps occurred at slightly higher temperatures in air compared to those in nitrogen.

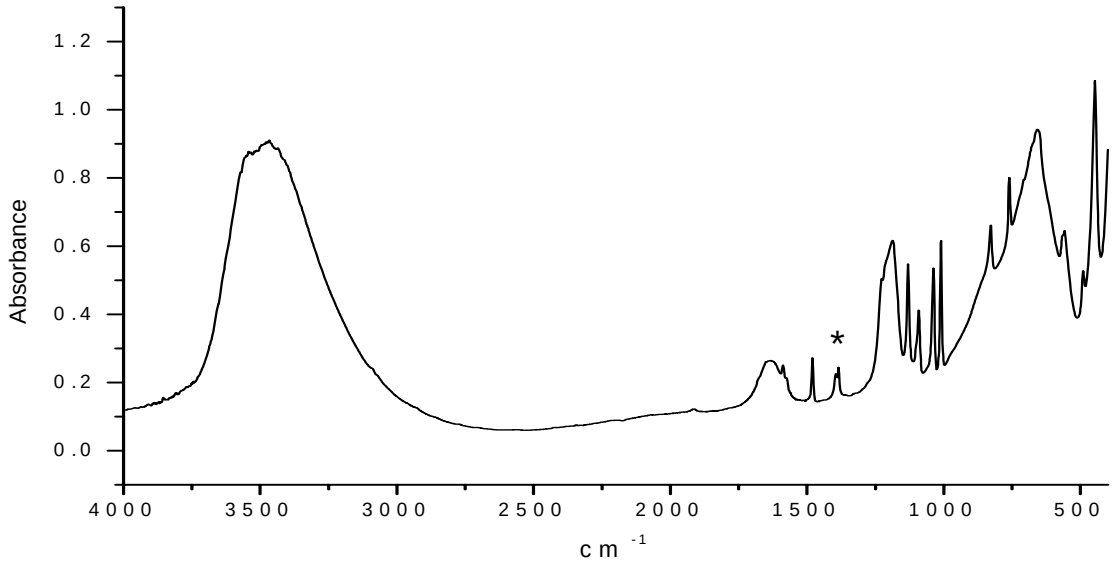

Figure.3.35: FTIR spectrum of 2:1 Mg-Al LDH 4-chlorobenzenesulfonate with nickel. Residual nitrate is indicated by the asterisk*.

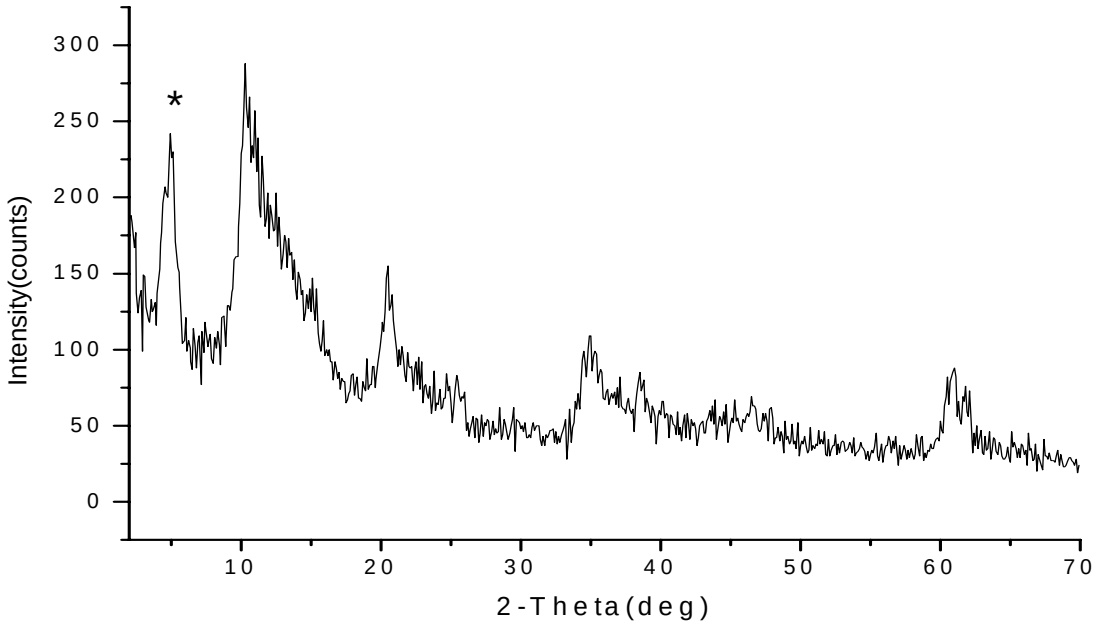

Figure 3.36: XRD pattern of 2:1 Mg-Al LDH 4-chlororbenzenesulfonate with nickel. d_{003} is indicated by the asterisk.

Table 3.11 XRD data for 2:1 Mg-Al LDH 4-chlorobenzenesulfonate with and without nickel.

2:1 Mg-Al LDH 4-chlorobenzenesulfonate	(003)	(006)	(009)	(0012)	(110/113)
Angle	5.00	10.27	15.36	20.66	60.81
d-spacing	17.35	8.6	5.76	4.29	1.52
2:1 Mg-Al LDH 4-chlorobenzenesulfonate with Ni:	(003)	(006)	(009)	(0012)	(110/113)
Angle	5.14	10.31	14.99	20.43	60.81
d-spacing	17.15	8.57	5.90	4.34	1.52

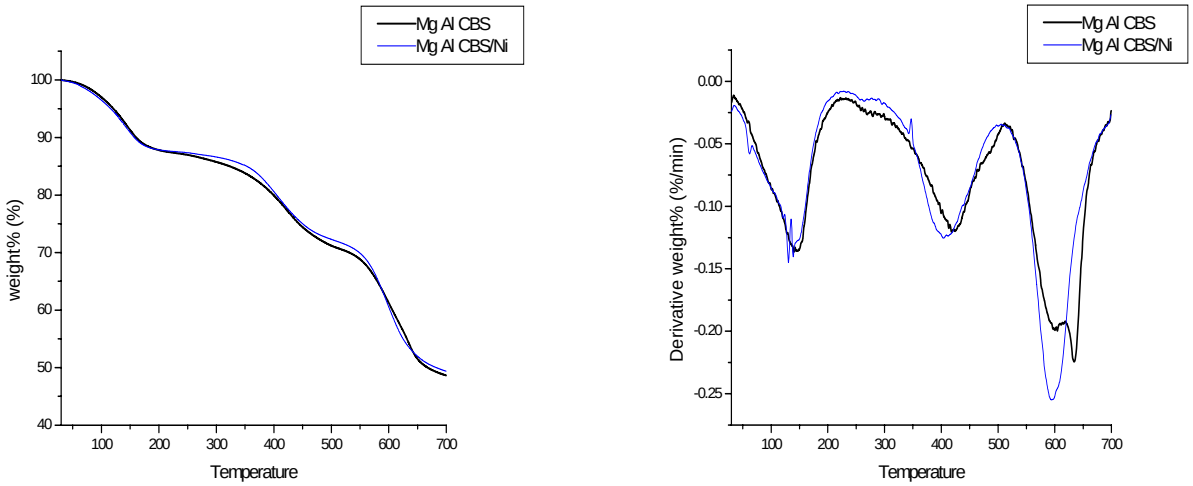

(a) (b)

Figure 3.37: (a) TGA comparison of 2:1 Mg-Al LDH 4-chlorobenzenesulfonate with and without nickel in nitrogen. (b) DTGA comparison of 2:1 Mg-Al LDH 4-chlorobenzenesulfonate with and without nickel in nitrogen.

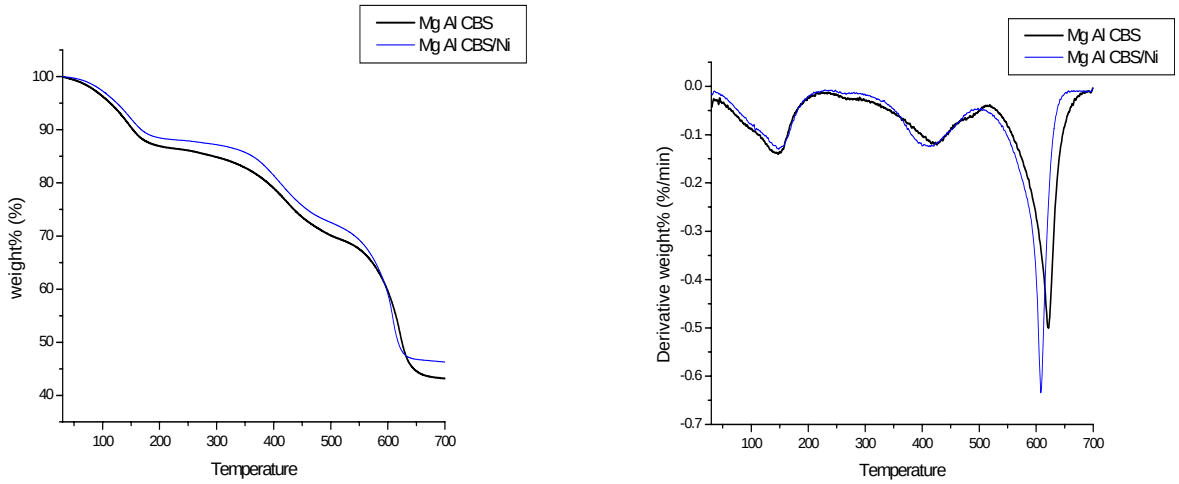

(a) (b)

Figure 3.38: (a) TGA comparison of 2:1 Mg-Al LDH 4-chlorobenzenesulfonate with and without nickel in air. (b) DTGA comparison of 2:1 Mg-Al LDH 4-chlorobenzenesulfonate with and without nickel in air.

b. 2:1 Zn-Al LDH 4-Chlorobenzenesulfonate

This material was prepared by exchanging 2:1 Zn-Al LDH nitrate with one mole of 4-chlorobenzenesulfonate per each mole of aluminum in the material. The infrared spectrum in the Figure 3.39 of the material again gives the proof of incorporation of the anion in that the 1384cm^{-1} peak which is indicative of interlayer nitrate is very much less in intensity compared to that in the infrared spectrum of nitrate precursor in Figure 3.13.Also the peak at 425 cm^{-1} is an indication for the presence of 2:1 Zn-Al LDH.

The XRD pattern in the Figure 3.41 with a d_{003} of 17.65 is a proof of the presence of 4-chlorobenzenesulfonate in the interlayer space. The complete list of tentative d-spacings is given in the Table 3.13.

The parent material when doped with nickel in this case also does not show any structural changes. The infrared spectrum and XRD pattern of the nickel doped material in Figures 3.40

and 3.42 when compared with those of the parent material prove this. Its d_{003} value of 17.36 compares well with that of the parent which is 17.65

Table 3.12 Atomic absorption and elemental analysis data for 2:1 Zn-Al LDH 4-chlorobenzenesulfonate with and without nickel:

LDH Sample	**%Zn**	**%Al**	**%Ni**	**Zn : Al**	**Zn : Ni**	**(Zn+Ni):Al**
Zn-Al CBS	26.8	5.5	-	2.0 : 1	-	2.0:1
Zn-Al CBS-Ni	26.8	5.5	0.09	2.0 : 1	273.7 : 1	2.0:1

LDH Sample	**%N_T**	**%N_E**	**%C_T**	**%C_E**	**%H_T**	**%H_E**	**%S_T**	**%S_E**
Zn-Al CBS	0.00	0.03	14.78	12.74	2.89	3.15	6.57	6.20
Zn-Al CBS-Ni	0.00	0.00	14.78	12.53	2.89	3.09	6.57	5.68

Table 3.13 XRD for 2:1 Zn-Al LDH 4-chlorobenzenesulfonate with and without nickel:

2:1 Zn-Al LDH 4-chlorobenzenesulfonate	(003)	(006)	(009)	(0012)	(0015)	(110/ 113)
Angle	5.00	10.18	15.30	20.51	25.71	60.48
d-spacing	17.65	8.68	5.79	4.33	3.46	1.53
2:1 Zn-Al LDH 4-chlorobenzenesulfonate with Ni:	(003)	(006)	(009)	(0012)	(0015)	(110/ 113)
Angle	5.08	10.37	15.38	20.71	25.73	60.45
d-spacing	17.36	8.52	5.75	4.28	3.45	1.53

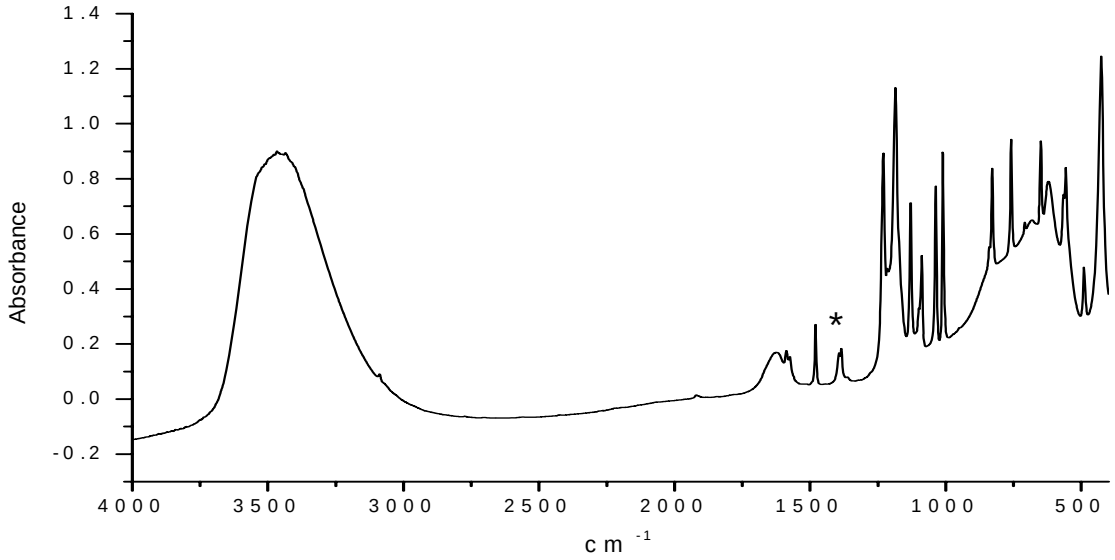

Figure 3.39: FTIR spectrum of 2:1 Zn-Al 4-chlorobenzenesulfonate. Residual nitrate is indicated by the asterisk*.

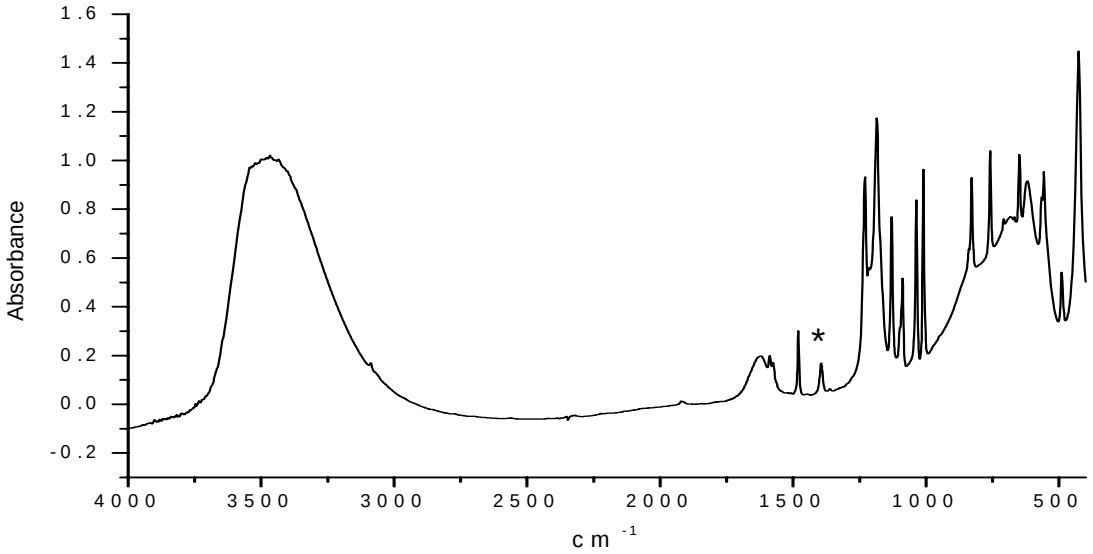

Figure 3.40: FTIR spectrum of 2:1 Zn-Al LDH 4-chlorobenzenesulfonate with nickel. Residual nitrate is indicated by the asterisk*.

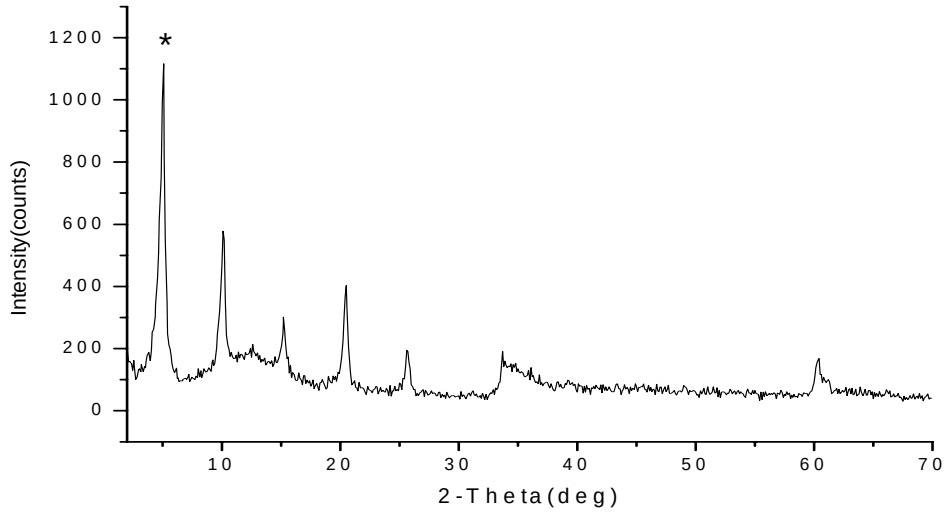

Figure 3.41: XRD pattern of 2:1 Zn-Al LDH 4-chlorobenzenesulfonate. d_{003} is indicated by the asterisk*.

Table 3.12 atomic absorption data show presence of nickel in the material even though no change is to be seen in the structure. The ratio of Zn to Al in the nickel doped material remained 2:1 owing to incorporation of very small amount of nickel. Table 3.12 elemental analysis data shows that the experimental values for the percentages agree well with their respective theoretical percentages.

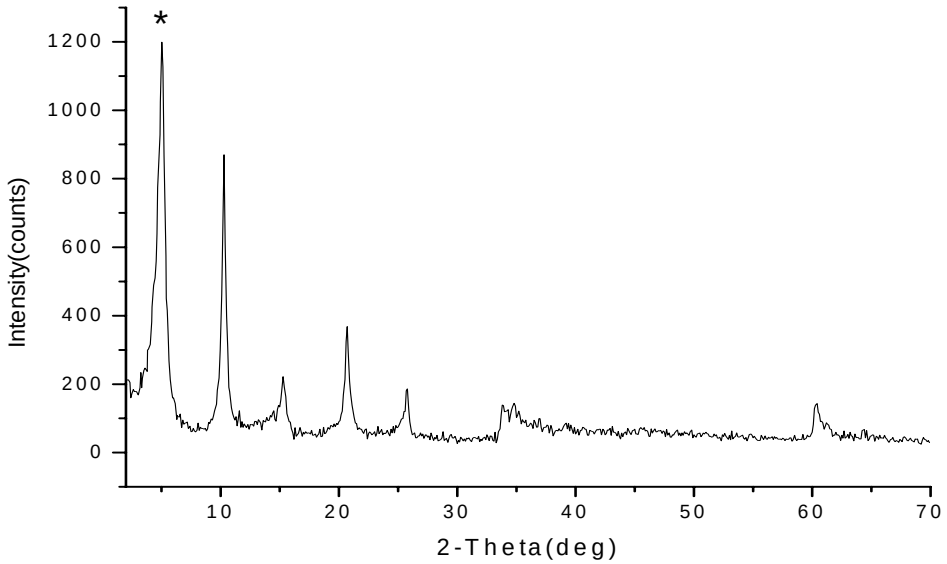

Figure 3.42: XRD pattern of 2:1 Zn-Al LDH 4-chlorobenzenesulfonate with nickel. d_{003} is indicated by the asterisk*.

The TGA and DTGA comparisons of the parent and nickel doped materials in the Figures 3.43 and 3.44 give evidence of the accelerated thermal decomposition when the material has nickel. There is no significant difference in the thermal behavior in nitrogen and air. The materials retained their original colors even after heat treatment in air i.e. the material with nickel was green, the color of nickel oxide and the one without nickel was white. Both the materials gave dark black residues upon TGA in nitrogen due to presence of char. The percent weight losses for materials with and without nickel in nitrogen are 48 and 47% and in air they are 57 and 57% respectively. The %weight of oxides of Zn and Al oxides which are the possible residues left after thermal treatment is about 48% and this agrees well with the experimental %weight losses. The weight loss steps occurred at about the same temperatures in air and nitrogen for both the materials.

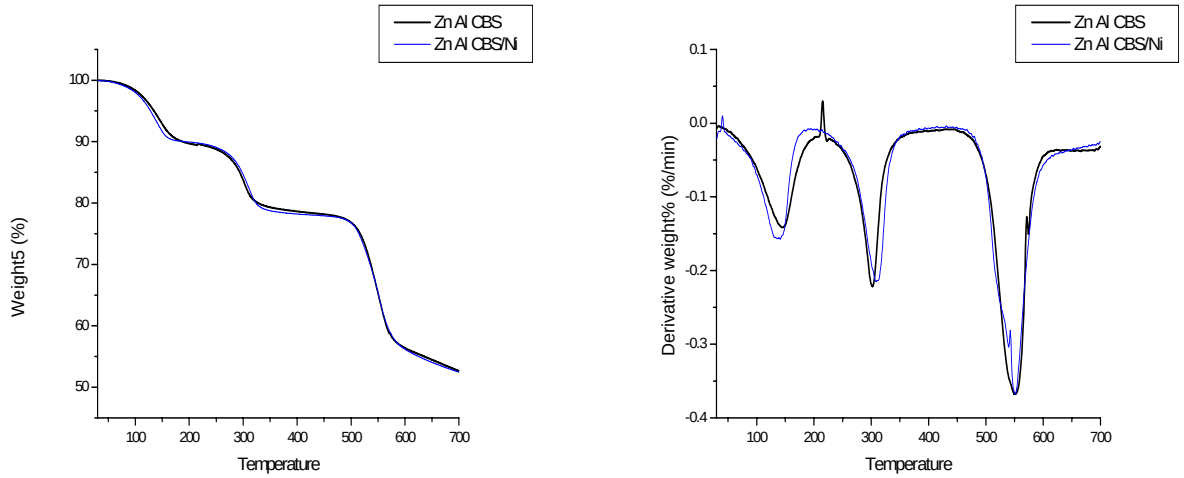

(a) (b)

Figure 3.43: (a) TGA comparison of 2:1 Zn-Al LDH 4-chlorobenzenesulfonate with and without nickel in nitrogen. (b) DTGA comparison of 2:1 Zn-Al LDH 4-chlorobenzenesulfonate with and without nickel in nitrogen.

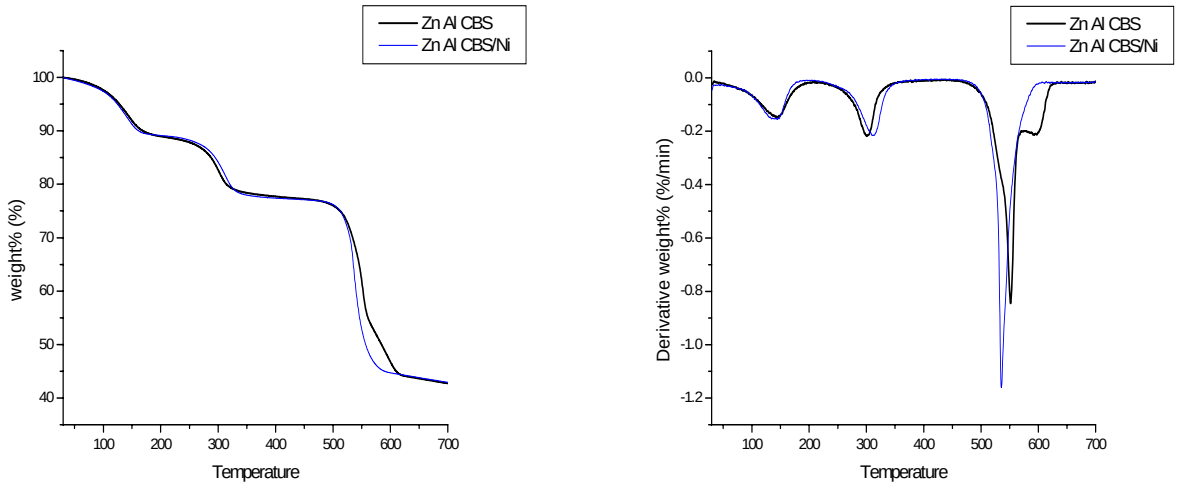

(a) (b)

Figure 3.44: (a) TGA comparison for 2:1 Zn-Al LDH 4-chlorobenzenesulfonate with and without nickel in air. (b) DTGA comparison for 2:1 Zn-Al LDH 4-chlorobenzenesulfonate with and without nickel in air.

3.5 Conclusions

1. The nitrate route of preparation of LDHs with sulfanilate, *p*-toluenesulfonate and 4-chlorobenzenesulfonate is a viable one as it gives good exchange and can also be stepped up the scale to make considerably large batches. 50gm samples of these materials were made in the procedure discussed above and the results were reproducible.

2. The same interlayer anions give better XRD patterns with zinc as the divalent metal when compared to magnesium, suggesting better structural properties.

3. The ratios of divalent to trivalent metal in zinc LDHs are closer to 2 compared to those in magnesium LDHs which also is an indication of their regular and predictable structure.

4. The drying of the materials after exchanging with the sulfonate anions did not require a vacuum to avoid carbonate from the air. This is an indication of their resistance to the carbonate contamination, which is desirable as well as profitable in the LDH chemistry.

5. Sulfanilate was needed in excess (twice the number of moles of LDH) to get a quantitative exchange whereas *p*-toluenesulfonate and 4-chlorobenzenesulfonate did not. This can be due to the fact that sulfanilate is poorly soluble in water, which makes lesser amount of the ion available for exchange at any given instant.

6. The incorporation and net exchange of nickel for a fraction of the divalent metal is an interesting result as this restricts the presence of nickel to small amounts which is expected to enhance its catalytic activity.

7. Zn Al LDHs also showed significantly less amounts of nickel doping compared to Mg Al LDHs which also makes zinc a better choice.

8. The weight loss on heating of these materials in air was found to require higher temperatures, in some cases only very slightly higher, compared to that in nitrogen. Mg Al LDH sulfanilate material is the only exception to this trend, in which the temperature required in nitrogen is slightly higher than that required in air for thermal decomposition.

9. The weight loss on heating of nickel-doped samples in the majority cases (except for the 2:1 Mg-Al LDH *p*-toluenesulfonate with nickel in air) is faster than their respective precursors. This illustrates nickel's catalytic role.

3.6 References

1. Carlino, S.; *Solid State Ionics.* **1997**, *98*, 73-84.
2. Meyn, M.; Beneke, K.; Lagaly, G. *Inorg. Chem.* **1995**, *5*, 1433-1442.
3. Chibwe, K.; Valim, J.B.; Jones, W. *Abstr.Pap. Am. Chem. Soc.* **1989**, *198*, 20-21.
4. Boehm, H.P.; Steinle, J.; Vieweger, C. *Angew Chem.* **1977**, *89*, 259-260.
5. Evans, W.H. *Spectrochimica Acta,* **1974**, *30A,* 543-547.

6. Kuwahara,T.; Ontisuka, O.; Tagaya, H. *Journal of inclusion phenomena and Molecular Recognition in chemistr* **1994**, *18*, 59-68.

7. Tagaya, H.; Sato, s.; Kuwahara, T.; Kadokawa, J.; Masa, K.; Chiba, K. *J, Mater. Chem.* **1994**, *4(12)*, 1907-1912.

8. Tagaya, H.; Sato, s.; Kuwahara, T.; Kadokawa, J.; Masa, K.; Chiba, K. *J, Mater. Chem.* **1994**, *4(12)*, 1907-1912.

9. Ballarin, B.; Gazzano, M.; Seeber, R.; Tonelli, D.; Vaccari, A. *Journal of electrochemical society,* **1998**, *445,* 27-37.

10. P. S. Braterman and Mickey C. Richardson, J. Phys. Chem. B, under revision.

11. JW Gilman, T Kashiwagi, M Nyden, JET Brown, CL Jackson, S Lomakin, EP Giannelis, E Manias, Chemistry and Technology of Polymer Additivies. Chapter 14. 1999, Blackwell Science Inc., Malden, MA.

12. Lakrami, M; Legrouri, A; Barroug, A.; De Roy, A.; Besse, J.P. *Mater, Res. Bull.* **2006**, *41* 1763.

CHAPTER 4

THE QUESTION OF HOMOGENEOUS PRECIPITATION

4.1 Introduction

Layered double hydroxides (LDHs) when prepared by the direct precipitation method or the copricipitation method or by any of the other conventional methods are less crystalline and have a very broad particle size range. Elevated temperatures and pressures of preparation have been found to increase the crystallinity of the material [1, 2]. A relatively recent method of preparing LDHs, called homogeneous precipitation, utilizes urea for the base in the neutralization of the solution of salts instead of sodium hydroxide, as discussed in chapter one [3].

The advantage of this method lies in the fact that urea hydrolyses progressively above 60^0C releasing ammonia via ammonium cyanate. This gradual release of base is the key difference between conventional preparative methods and the homogeneous method. In the conventional methods when all the required base is made available in the solution the nucleation and particle growth steps in the crystal formation overlap leading to broad distribution of particle size [4]. Urea has been used to synthesize metal oxides and carbonates of uniform particle size before [5-9]. LDHs of different compositions were also made by the urea method [3, 10-12].

Ogawa et al. [13] combined this technique with increased temperature and pressure method, commonly referred to as hydrothermal treatment to obtain particles of better crystallinity and bigger particle sizes.

The reaction by which urea releases ammonia [14] is as follows:

$$CO(NH_2)_2 \longrightarrow NH_4CNO$$

$$NH_4CNO + 2H_2O \longrightarrow (NH_4)CO_3$$

Recently Iyi et al. [15] claimed homogeneous precipitation of layered double hydroxide with hexamethylenetetramine (HMTA) as the base. The 2:1 Mg-Al LDH CO_3 they made by hydrothermal treatment of magnesium and aluminum chlorides along with HMTA was of superior crystallinity. We set out to verify this observation and found some interesting facts about the use of HMTA in LDH chemistry.

4.2 Starting Materials Used

The starting materials used for this study are all used as they were bought from the manufacturers. Table 4.1 gives of the chemicals used along with their grades. The deionized water used was freshly prepared from 'Milli-Q academic' (18MΩ cm^{-1}).

Table 4.1: Chemicals used for the synthesis of compounds studied and their sources.

Name	Grade	Supplier
$Al(NO_3)_3.9H_2O$	98.0-102%	Alfa Aesar
$Mg(NO_3)_2.6H_2O$	98%	Alfa Aesar
$Zn(NO_3)_2.6H_2O$	98%	Sigma-Aldrich
$Cr(OH)_3.9H_2O$	99%	Aldrich
Hexamethylenetetramine	ACS, 99+%	Alfa Aesar

4.3 Principle

Every mole of hexamethylenetetramine is believed to give four ammonium ions which in turn produce four hydroxyl groups from the relationship given below.

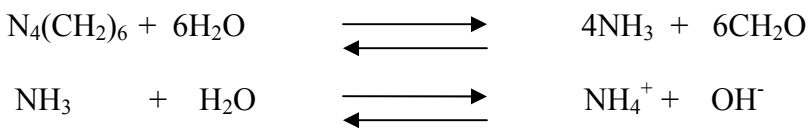

So, for each mole of 2:1 LDH, 1.5 mole of HMTA was required to supply six hydroxides.

Three different combinations of metals were studied for the experiment. They are 2:1 Mg-Al LDH, 2:1 Zn-Al LDH and 2:1 Zn-Cr LDH. For the materials containing Al the titration curve with sodium hydroxide shows two plateaus of which the first one corresponds to the formation of aluminum hydroxide, which always forms as an intermediate in the synthesis of Al containing LDH and the second one corresponds to the formation of LDH [16-19]. The Cr(III) containing LDH on the other hand shows just one plateau which corresponds to the formation of LDH, the step which occurs at a pH less than what is needed to precipitate either $Cr(OH)_3$ or the divalent metal hydroxide [20].

Two different concentrations of HMTA were tested with the above divalent and trivalent metal combinations. The first one was with 1.5 moles of HMTA per each mole of trivalent metal in the LDH so that the reaction proceeds to completion. The second one was with 0.75 moles of HMTA per each mole of trivalent metal in the LDH so that only half the amount of base is available for the neutralization, which should produce half the calculated amount of LDH and half of the starting materials would remain in the product, if, the reaction is indeed homogeneous. If the reaction is not homogeneous and proceeds via an intermediate like aluminum hydroxide, as the Al containing LDHs do when treated with sodium hydroxide, we expected to find only this intermediate and no LDH as there was enough base only to carry the reaction that far.

4.4 Synthesis

For the synthesis of LDHs the divalent and trivalent metal nitrates were dissolved together in 40ml of deionized water in concentrations of 0.3M and 0.1M respectively and a 20ml solution of HMTA containing 1.5M of HMTA per each mole of trivalent metal was added to it to for the intended preparation of 1gm of LDH. For the second set of experiments in which half the amount of HMTA was used, the concentrations of metal salts was kept the same and a solution of only 0.75M of HMTA per each mole of trivalent metal is added to it. In both the cases the mixture was stirred thoroughly for 10min under nitrogen and then it was transferred into Parr general purpose acid digestion bombs of 45ml capacity and heated in a hot air oven for 24hr at a temperature of 130^0-140^0C.

Upon completion of 24hr the hydrothermal containers were taken out of the oven and were allowed to cool in an ice bath. The resultant slurries were centrifuged to obtain the suspended solid and the supernatant liquid was also stored for further examination. The solids thus obtained were washed twice with deionized water by centrifugation, dried in a desiccator and stored.

4.5 Results

4.5.1 Magnesium and Aluminum Nitrates with HMTA

The product obtained upon hydrothermal treatment of a solution of magnesium and aluminum nitrates with 1.5M HMTA per each mole of Al was a suspension, which gave a white powder on washing and drying. The Figure 4.1 shows the infrared spectrum of the material collected. It resembles the typical infrared spectrum of a 2:1 Mg-Al LDH CO_3 with the peak around 447cm^{-1} indicative of 2:1 ratio of Mg and Al and the peak around 1360cm^{-1} indicative of

carbonate anion. The shoulder observed for the –OH stretching mode at 3300cm^{-1}, around 3100cm^{-1} of infrared spectrum is because of hydrogen bonding between the carbonate and the interlayer water molecules is also a proof of presence of carbonate.

The XRD pattern of the material depicted in Figure 4.2 also confirms the presence of well crystalline material that has a d-spacing of 7.63 which corresponds well to carbonate. The d_{110} and d_{113} peaks are also well resolved owing to the superior crystallinity of the material. The XRD pattern also shows some additional peaks which can be assumed to be those of the other hydrolysis products of HMTA which contaminate the material and are hard to separate. The full d-spacings of the pattern are given in Table 4.2.

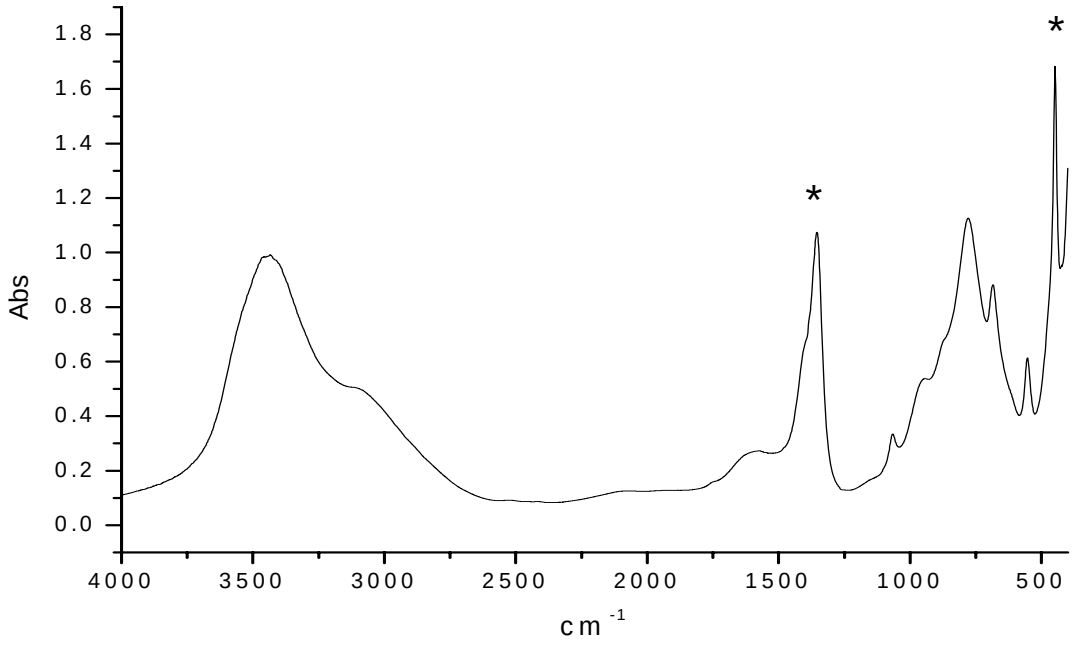

Figure 4.1: FTIR spectrum of the material synthesized by treating Mg and Al nitrates with 1.5M HMTA per each mole of Al. Carbonate peak and the 447cm^{-1} peak are indicated by asterisk*.

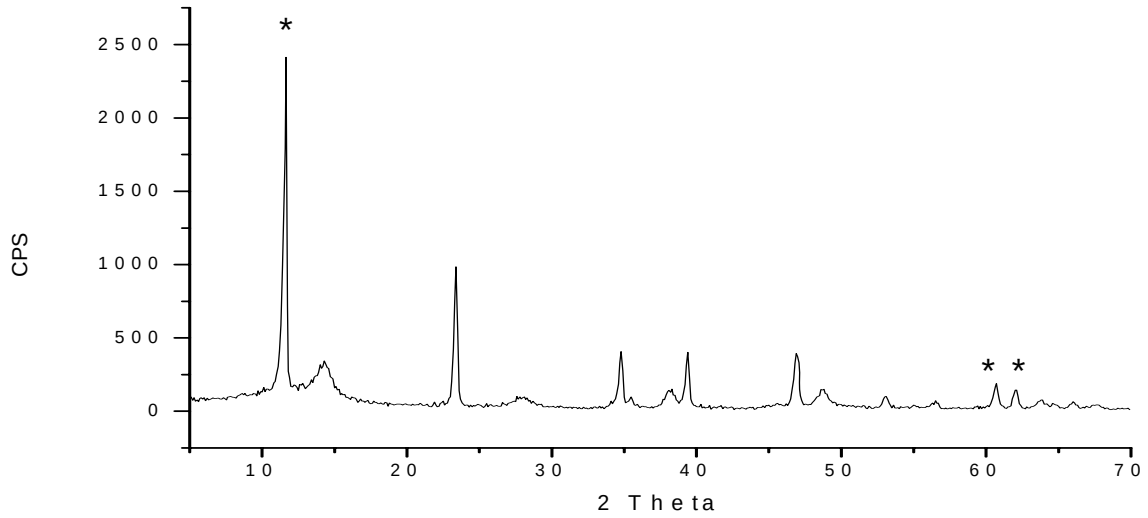

Figure 4.2: XRD pattern of the material synthesized by treating Mg and Al nitrates with 1.5M HMTA per each mole of Al. d_{003}, d_{110} and d_{113} peaks are indicated by asterisks*.

Table 4.2 XRD data for material synthesized by treating Mg and Al nitrates with 1.5M HMTA per each mole of Al:

	(003)	(006)	(009/012)	(015)	(018)	(110)	(113)
Angle	11.59	23.40	34.81	39.40	46.96	60.71	62.09
d-spacing	7.63	3.79	2.57	2.28	1.93	1.52	1.49

The ratio of magnesium and aluminum in the material was calculated by obtaining concentrations of individual metals in it employing atomic absorption spectroscopy and the results are given in Table 4.3 along with the ratio of metals in the supernatant liquid. The magnesium to aluminum ratio in the material was 1.02:1, which is about one half of the expected value. The ratio in the supernatant liquid, which though not a very accurate measurement owing to the high concentration of Mg and very low concentration of Al was 232.96:1 which is reasonable as the amount of excess magnesium taken initially to make the LDH is expected to remain in the solution. A 3:1 ratio of Mg:Al was taken initially for preparing a 2:1 Mg-Al LDH

NO_3 because the excess of magnesium is believed to be acting as a buffer for the changes in the pH occurring during LDH formation.

The reduced amount of HMTA, i.e, 0.75M HMTA per each mole of Al also gave a suspension of a white solid. The infrared spectrum of the product is shown in Figure 4.3 which does not have the characteristic peaks of a 2:1 Mg-Al LDH like a peak at 445 cm^{-1}. It shows the peaks between 400 and 800 cm-1 which are indicative of metal-O bonds, which suggests that the product is a metal oxide or hydroxide of aluminum or magnesium or a mixture of any of these.

Table 4.3 Atomic absorption results for the materials synthesized by treating Mg and Al nitrates with HMTA.

Reactants	Mg:Al ratio
Mg Al Nitrates with 1.5 HMTA per each Al	1.02
Supernatant Mg Al Nitrates with 1.5 HMTA per each Al	232.96
Mg Al Nitrates with 0.75 HMTA per each Al	0.01
Supernatant Mg Al Nitrates with 0.75 HMTA per each Al	193.25

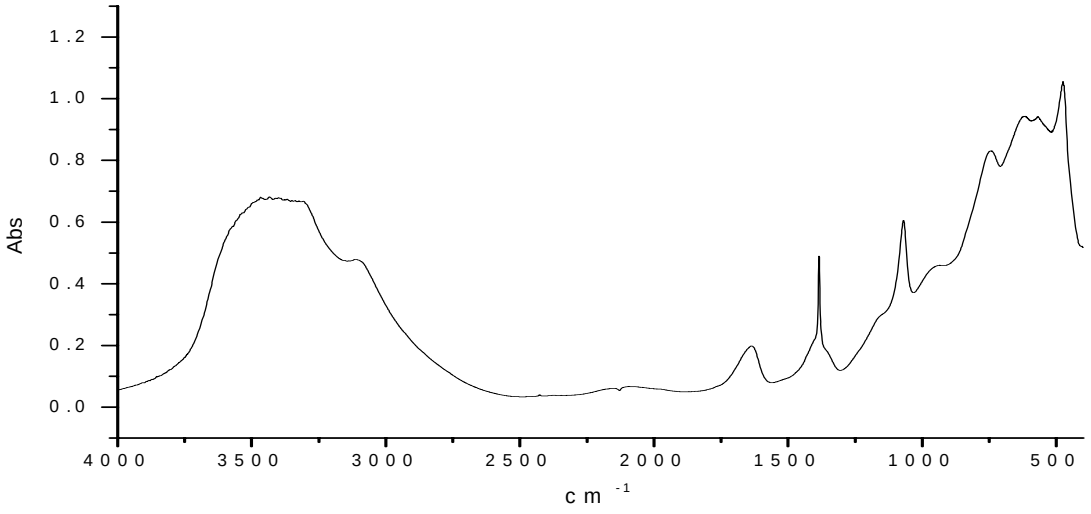

Figure 4.3: FTIR spectrum of the material synthesized by treating Mg and Al nitrates with 0.75M HMTA per each mole of Al.

The Figure 4.4 shows the XRD pattern of this material which is not typical of LDH again and this is consistent with the infrared observation. The twin peaks at the 2theta value of 60^0 which are typical of any LDH are not to be found and this evidence is conclusive enough to rule out the presence of LDH.

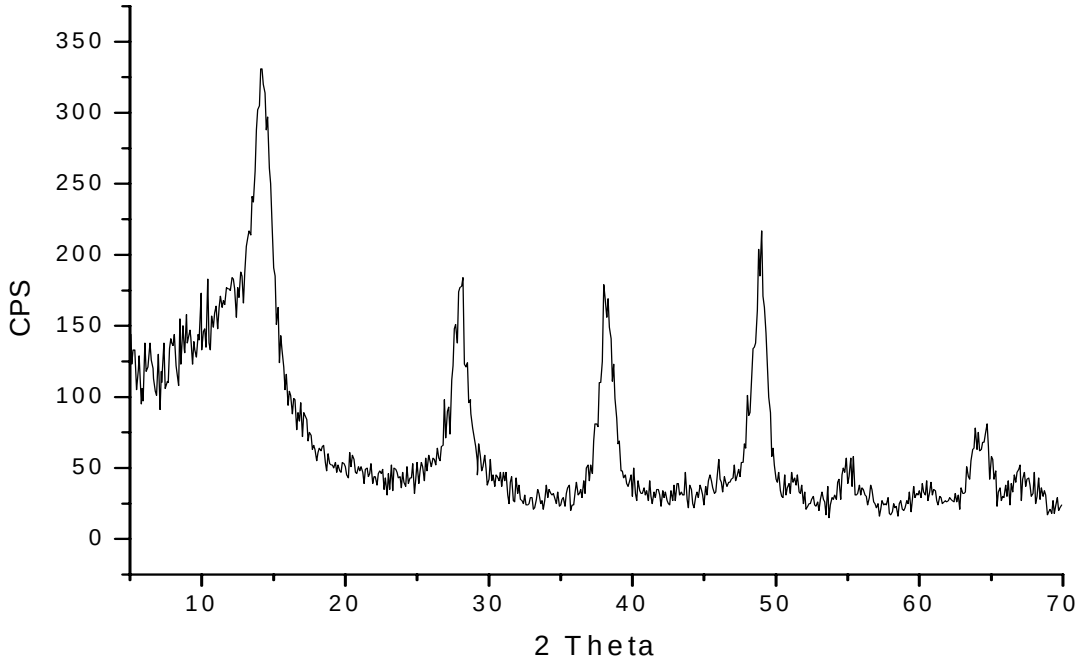

Figure 4.4: XRD pattern of the material synthesized by treating Mg and Al nitrates with 0.75M HMTA per each mole of Al.

The metals ratio in the solid and the supernatant liquid are presented in the Table 4.3. The ratio of Mg to Al in the solid which is 0.01:1 is reflective of the fact that there is practically no magnesium in the solid and it is a combination of hydroxides of aluminum. The ratio of 193.25:1 of Mg:Al in the supernatant again shows a lot excess of magnesium in it which is expected, a there is no incorporation of magnesium in the solid to form LDH.

4.5.2. Zinc and Aluminum Nitrates with HMTA:

A solution of zinc and aluminum nitrates added with a solution of HMTA which

contained 1.5M HMTA per each mole of Al or with 0.75M of HMTA per each mole of Al when treated hydrotheramlly for 24hr at 130-140^{0}C gave a suspension of a white solid which was washed and dried for examination. The supernatant collected was also analyzed for the metal concentrations.

Figure 4.5 shows the infrared spectrum of the solid and it contains all the peaks corresponding to 2:1 Zn-Al LDH like the peaks at 425cm^{-1} indicating the 2:1 ratio of Zn:Al, the metal-O bonds are indicated by the peaks from 400- 800cm^{-1} and it shows a peak at 1384cm^{-1} which has a shoulder indicating presence of some carbonate. The infrared spectrum in the Figure 4.7 is of the material prepared by using 0.75M HMTA per each mole of Al. It does not have the peak around 425cm^{-1} which suggests that we may not have got LDH. Again The M-O bonds

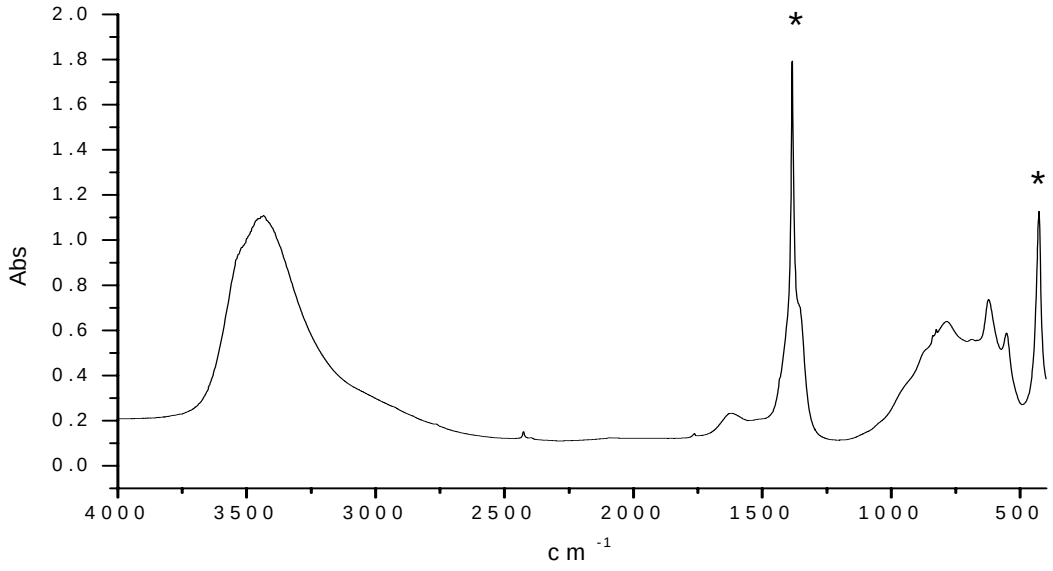

Figure 4.5: FTIR spectrum of the material synthesized by treating Zn and Al nitrates with 1.5M HMTA per each mole of Al. Carbonate/ Nitrate peak and 425cm^{-1} peak are indicated by the asterisk*.

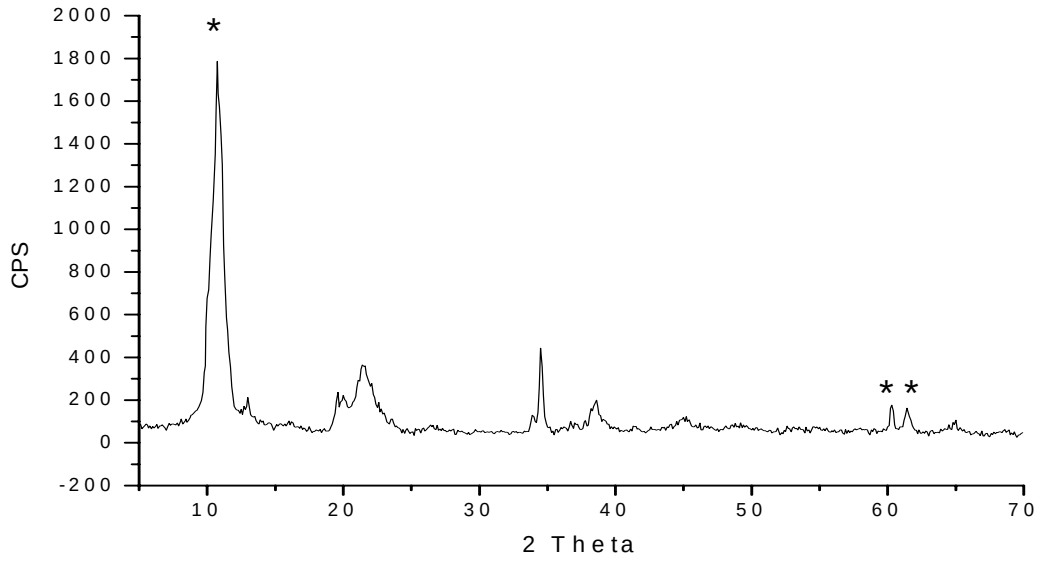

Figure 4.6: XRD pattern of the material synthesized by treating Zn and Al nitrates with 1.5M HMTA per each mole of Al. d_{003}, d_{110} and d_{113} are indicated by asterisks*.

Table 4.4 XRD data for the material synthesized by treating Zn and Al nitrates with 1.5M HMTA per each mole of Al:

	(003)	(006)	(009/012)	(015)	(018)	(110)	(113)
Angle	10.80	21.42	34.59	38.51	45.10	60.33	64.99
d-spacing	8.18	4.14	2.59	2.33	2.00	1.53	1.43

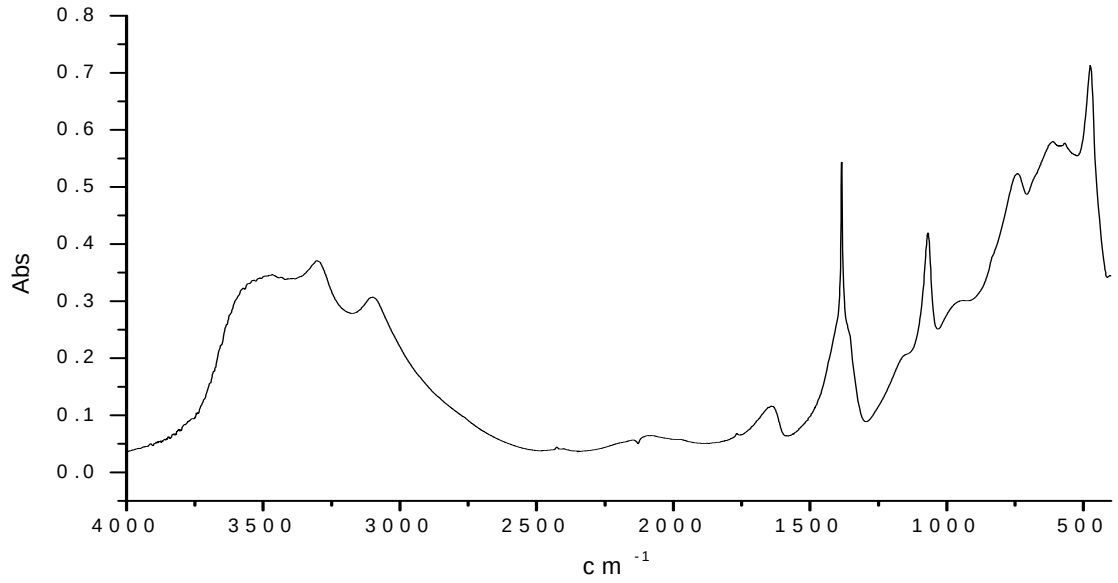

Figure 4.7: FTIR spectrum of the material synthesized by treating Zn and Al nitrates with 0.75M HMTA per each mole of Al.

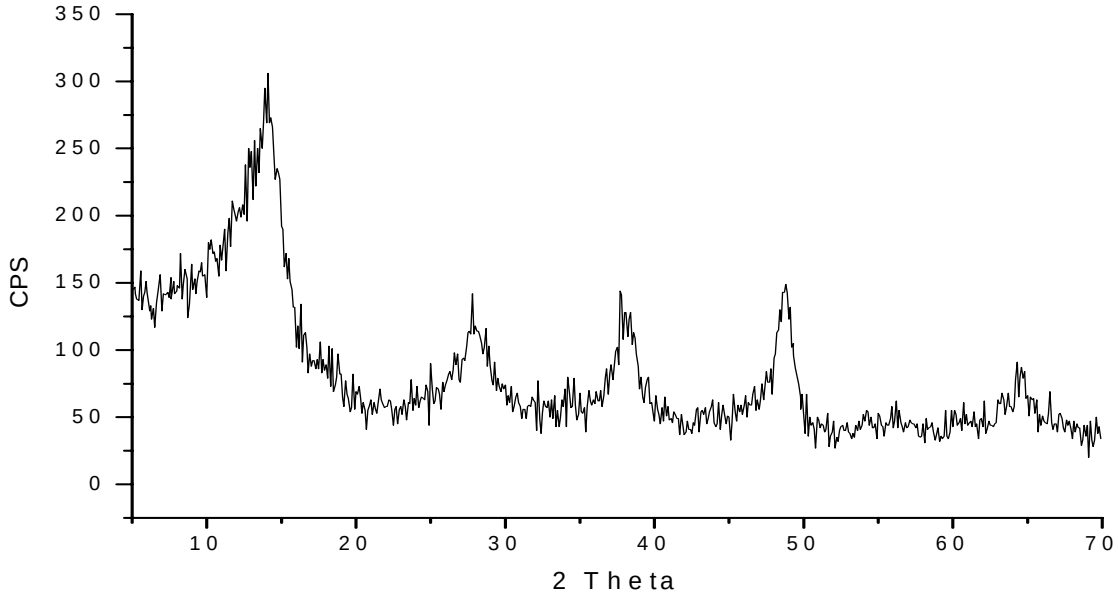

Figure 4.8: XRD pattern of the material synthesized by treating Zn and Al nitrates with 0.75M HMTA per each mole of Al.

between 400-800cm^{-1} are there and the spectrum looks a lot similar to the spectrum obtained by treating Mg and Al nitrates with 0.75M HMTA.

The XRD patterns of both the materials are given in the Figures 4.6 and 4.8. The material with 1.5M HMTA in Figure 4.6 shows a pattern of an LDH with sharp peaks at about 60^0 2theta. A Complete list of d-spacings for it are given in the Table 4.4 The pattern of material with 0.75 HMTA in Figure 4.8 on the other hand has no peaks characteristic of LDH including the ones at 60^0 2theta. Again, it is similar to the XRD pattern of the material obtained from treating Mg and Al nitrated with 0.75 HMTA.

The Zn:Al ratios in both the materials in solid and also in the supernatant liquid are given in the Table 4.5. The ratio for the material treated with 1.5M HMTA is 1.60:1 for the solid which is not quite the expected value of 2:1. The ratio in the supernatant of the same material is 151.08:1, also not a very accurate measurement due to large disparity in the concentrations of metals in it, can be explained by the excess of Zn taken in initially.

For the solid prepared by using the 0.75M HMTA the ratio of Zn to Al was found to be 0 which means that there is no zinc in the solid whatsoever. The ratio in the supernatant of the same material is 121.12:1 which is again on the expected lines.

Table 4.5 Atomic absorption results for the materials synthesized by treating Zn and Al nitrates with HMTA.

Reactants	Zn:Al ratio
Zn Al Nitrates with 1.5 HMTA per each Al	1.60
Supernatant Zn Al Nitrates with 1.5 HMTA per each Al	151.08
Zn Al Nitrates with 0.75 HMTA per each Al	0
Supernatant Zn Al Nitrates with 0.75 HMTA per each Al	121.12

4.5.3. Zinc and Chromium Nitrates with HMTA

Again a 40ml combination of zinc and chromium nitrates solutions with 0.3M Zn and 0.1M Cr was mixed with 20ml 1.5M and 0.75M HMTA solutions separately and was treated hydrothemally for 24hr at a temperature of around 130-140^{0}C. The solid obtained in the first case was pale green to grey in color and the one in the second case was green in color.

The infrareds of both the solids are given in the Figures 4.9 and 4.11. The figure 4.9 is the IR of the material with 1.5M HMTA and it shows the peak around 507cm^{-1} which is indicative of 2:1 Zn-Cr LDH and the M-O vibrational peaks are also present between 400 and 800cm^{-1}. The spectrum of the material with 0.75M HMTA in Figure 4.11 shows a broad peak at 515cm-1 which may be due to the presence of a trace of 2:1 Zn-Cr LDH.

The XRD pattern of the 1.5M HMTA material in Figure 4.10 indicates a material less crystalline compared to those obtained by treating Mg Al and Zn Al nitrates with 1.5M HMTA. It however has the twin peaks around 60^0 2theta which indicate presence of LDH. A complete list of d-spacings for this pattern is given in Table 4.6. The material with 0.75M HMTA has pattern looking more like an amorphous material than any LDH as it has no prominent and distinguishable peaks. It is given in the Figure 4.12.

The metal ratios in the solid and the supernatant liquid are presented in the Table 4.7. The solid in the case of 1.5M HMTA material has a Zn to Cr ratio of 1.16:1 which is again less than the expected value of 2:1. The supernatant of this material is found to have a ratio of 5646.12:1 for Zn:Cr which means there is a large excess of Zn in it which is expected because of the excess of Zn added to the reactant vessel.

The metal ratio in the solid obtained by treating the Zn and Cr nitrates with 0.75M HMTA per each mole of Cr has a Zn;Cr ratio of 0.25:1 which means that there is a small amount

Table 4.6 XRD data for material synthesized by treating Zn and Cr nitrates with 1.5M HMTA per each mole of Cr.

	(003)	(006)	(009/012)	(015)	(110)	(113)
Angle	11.64	23.47	34.59	38.59	60.68	64.60
d-spacing	7.59	3.79	2.59	2.33	1.52	1.44

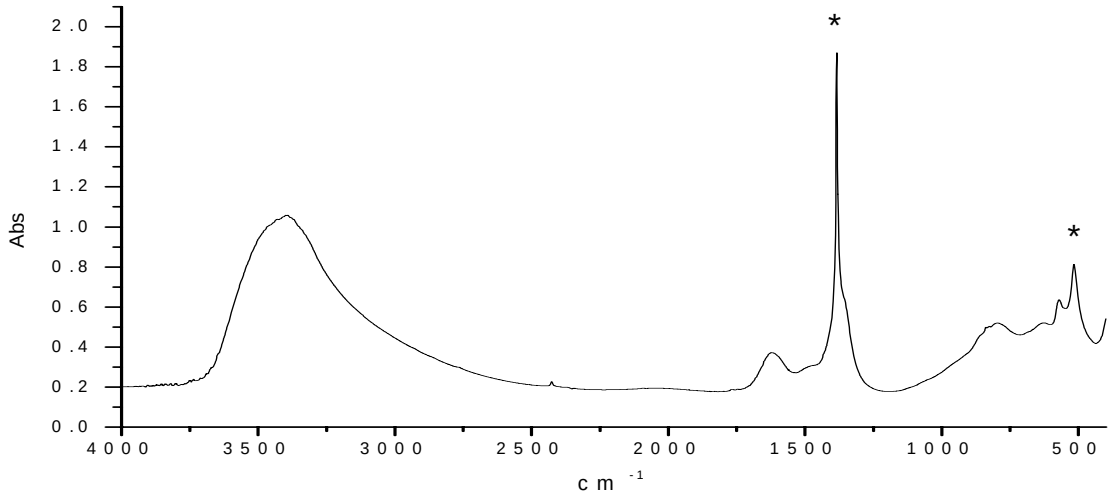

Figure 4.9: FTIR spectrum of the material synthesized by treating Zn and Cr nitrates with 1.5M HMTA per each mole of Cr. Nitrate/carbonate peak and 507m^{-1} peak are indicated by asterisks*.

of zinc in the material which can be expected to be in the form of LDH along with Cr. This assumption is strengthened by the fact that the infrared of this material shows a broad peak at 515cm^{-1} which can be because of the 2:1 Zn-Cr LDH. The supernatant of this material has a Zn: Cr ratio of 11779.32:1 again a number not very much accurate but gives a fair approximation of the large difference in concentration of the metals in the solution.

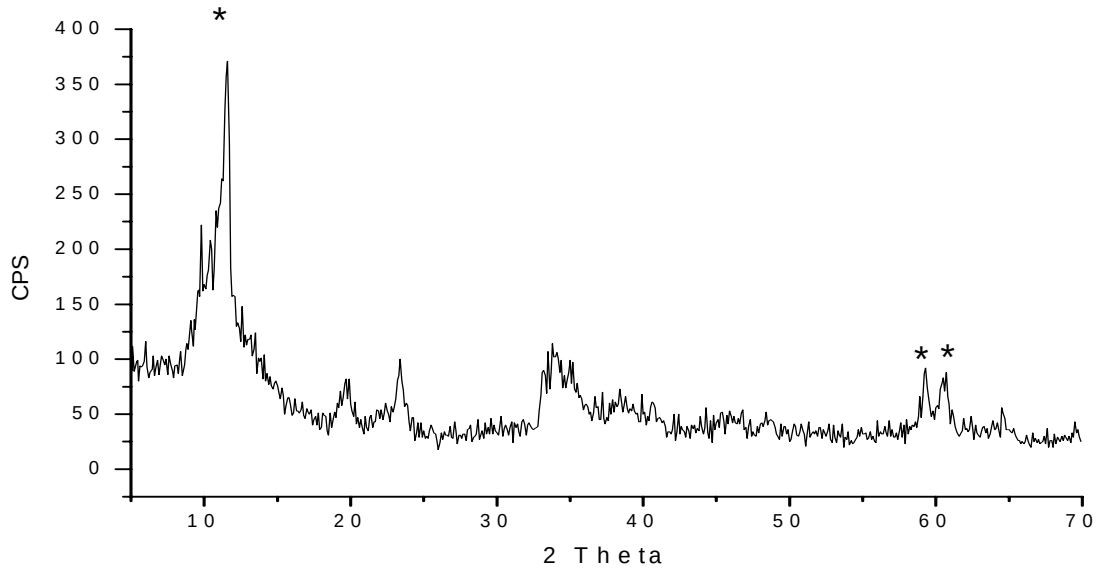

Figure 4.10: XRD pattern of the material synthesized by treating Zn and Cr nitrates with 1.5M HMTA per each mole of Cr.d_{003}, d_{110} and d_{113} are indicated by asterisks*.

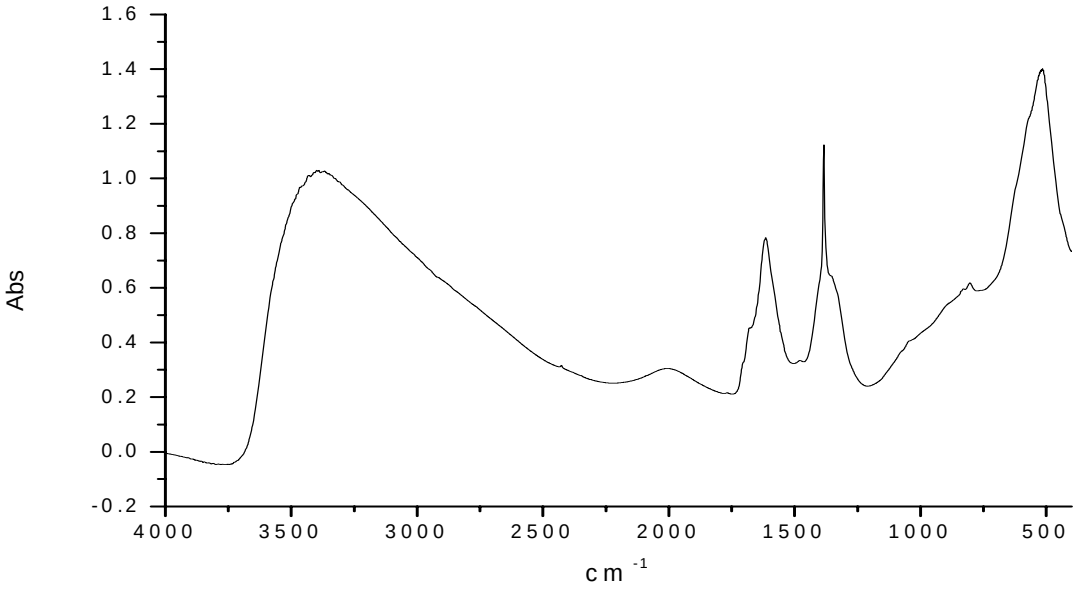

Figure 4.11: FTIR spectrum of the material synthesized by treating Zn and Cr nitrates with 0.75M HMTA per each mole of Cr.

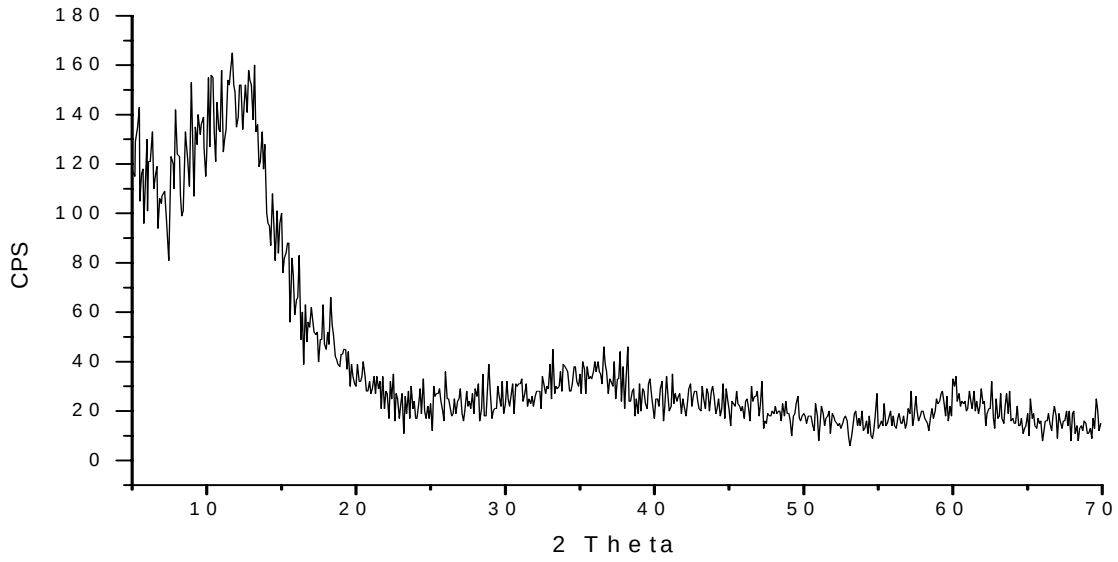

Figure 4.12: XRD pattern of the material synthesized by treating Zn and Cr nitrates with 0.75M HMTA per each mole of Cr.

Table 4.7 Atomic absorption results for the materials synthesized by treating Zn and Cr nitrates with HMTA.

Reactants	Zn:Cr ratio
Zn Cr Nitrates with 1.5 HMTA per each Cr	1.16
Supernatant Zn Cr Nitrates with 1.5 HMTA per each Cr	5646.12
Zn Cr Nitrates with 0.75 HMTA per each Cr	0.25
Supernatant Zn Cr Nitrates with 0.75 HMTA per each Cr	11779.32

4.6 Conclusions and Suggestions for Future Work

4.6.1 Conclusions

1) The ratios of divalent metal to trivalent metal in the materials produced by using 1.5M HMTA per each mole of trivalent metal are all consistently lower than the expected value of 2:1. This can be due to the fact that the amount of base (ammonia) released by the HMTA is less than the expected value which can be due to partial hydrolysis of formaldehyde, which forms as an intermediate in the HMTA hydrolysis [21].

2) The solids obtained in the case of Mg Al and Zn Al systems contained very low to no amount of divalent metal when half the amount of HMTA needed for LDH formation (0.75M) was used. This indicated the formation of an intermediate compound of the trivalent metal, which suggests that the HMTA route is not homogenous.

3) The solid obtained when Zn and Cr nitrates were treated with 0.75M HMTA has some appreciable amount of Zn which can be explained by the fact that the LDH formation for Zn Cr systems is direct without the involvement of chromium hydroxide intermediate. The ratio of Zn:Cr however less than the expected value of 1:1 here, which can again be explained by the claim of disproportionation of formaldehyde formed as intermediate in the hydrolysis of HMTA..

4) The solids obtained by treating Mg Al and Zn Al systems with 0.75M HMTA have identical infrared spectra and their XRD patterns were also similar. This is a proof that both the materials are compounds of aluminum only. This supports the assumption that aluminum compounds indeed form as the intermediate in both the cases.

5) The formation of aluminum hydroxide as concluded in points 2 and 4 and the formation of a small amount of LDH in the case of Zn Cr system as concluded in point 3 lead us

to claim that the process of formation of LDH in both the cases is by the conventionally established pathways and is not by homogeneous precipitation.

6) Homogeneous precipitation would result in formation of half the stiochiometric amount of LDH in the case of materials treated with 0.75M HMTA, i.e we would have got half the amount of LDH got in the case of 1.5M HMTA in the 0.75M HMTA experiment. But this did not happen and the absence of divalent metal in the 0.75M HMTA in Mg Al and Zn Al is proof enough for this.

7) The superior crystallinity of the materials obtained when 1.5M HMTA can be because of the elevated temperature employed rather than the homogenous precipitation.

8) We finally conclude that the formation of LDH in HMTA method may not be by homogenous precipitation.

4.6.2 Suggestions for Future Work

1) The products in the case of Mg Al and Zn Al treatment with 0.75M HMTA can be analyzed to establish their chemical identity, which would throw some more light on the processes occurring during LDH formation.

2) The assumption of partial hydrolysis of HMTA can be verified by increasing the amount of HMTA in the experiments where complete formation of LDH is expected (1.5M HMTA per each Al can be increased to 2 or 2.5 and the products can be studied).

3) Urea method of homogeneous precipitation can be repeated with half the amount of urea required for the formation of LDH and the products be studied to see the similarities and differences between that and the HMTA method.

4) The experiments can be conducted with chlorides of metals instead of nitrates to see what, if any effects the anion has on the mechanism of LDH formation in HMTA method.

4.7 References

1. Reichle, W.T. *Solid State Ionics* **1986**, *22*, 135.
2. Cavani, F.; Trifiro, F.; Vaccari, *Catal. Today* **1991**, *11*, 173.
3. Costantino, U.; Marmottini, F.; Nocchetti, M.; Vivani, R. *Eur. J. Inorg. Chem.* **1998**, 1439-1446.
4. Adchi-Pagano, M.; Forano, C.; Besse, J.P. *J. Mater. Chem.* **2003**, *13*, 1988-1993.
5. Willard, H.H.; Tang, N.K. *J. Am. Chem. Soc.* **1937**, *59*, 1190.
6. Sordelet, D.; Akinc, M. *J. Colloid Interface Sci.* **1988**, *122*, 47.
7. Matevic, E.; Hsu, W.P.; *J. Colloid Interface Sci.* **1987**, *118*, 506.
8. Ocana, M.; Morales, M.P.; Serna, C.J. *J. Colloid Interface Sci.* **1999**, *212*, 317.
9. Wang, L.; Sondo, I.; Matijevic, E. *J. Colloid Interface Sci.* **1999**, *218*, 545.
10. Narita, E.; Matsuna, Y.; Takahashi, S.; Umetsu, Y. *J. Chem. Soc. Jpn.* **2001**, *5*, 273.
11. Cai, H.; Hillier, A.C.; Francklin, K.R.; Nunn, C.C.; Ward, M.D. *Science*, **1994**, *266*,1551.
12. Costantino, U, Coletti, N.; Nocchetti, M.; Aloisi, G.G.; Elisei, F.; Latterini, L. *Langmuir,***2000**, *16*, 10351.
13. Ogawa, M.; Kaiho, H. *Langmuir,* **2002,** *18*, 4240-4242.
14. Shaw, W. H. R.; Bordeaux, J.J. *J. Am. Chem. Soc.* **1955**, *77*, 4729.
15. Iyi, N., Matsumoto, T.; Kaneko, Y.; Kitamura., K. *Chemistry letters*, **2004**, *11*, 1122.
16. Cavani, F.; Trifiro, F.; Vaccari, A.; *Cat. Today.* **1991**, *11*, 173-301.
17. Boclair, J.W.; Braterman, P.S. *Chem. Mater.* **1999**, *11*, 298-302.
18. de Roy, A.; Forano, C.; El Malki, K.; Besse, J.P. *Expanded Clays and Other Microporous Solids*. New York:Reinhold, **1992**, pp 108-169.

19. Boclair, J.;Themodynamic and structural studies of layered double hydroxides. PhD Dissertation, University of North Texas, Denton, Tx, **1998**.

20. Boclair, J.W.; Braterman, P.S.; Jiang. J.; Lou, S.; Yarberry, F. *Chem. Mater.* **1999**, *11*, 303-308.

21. Marooka, S.; Wakai, C.; Matubayasi, N.; Nakahara, M.; *Journal of Physical Chemistry A*, **2005**, *109(29)*, 6610-6619.